Dual Noncanonical Amino Acid Incorporation Enabling Chemoselective Protein Modification at Two Distinct Sites in Yeast

Priyanka Lahiri[1] and James A. Van Deventer[1,2]*
[1]Chemical and Biological Engineering Department, Tufts University, Medford, MA 02155, USA
[2]Biomedical Engineering Department, Tufts University, Medford, Massachusetts 02155, USA

*Correspondence: james.van_deventer@tufts.edu

Graphical Abstract:

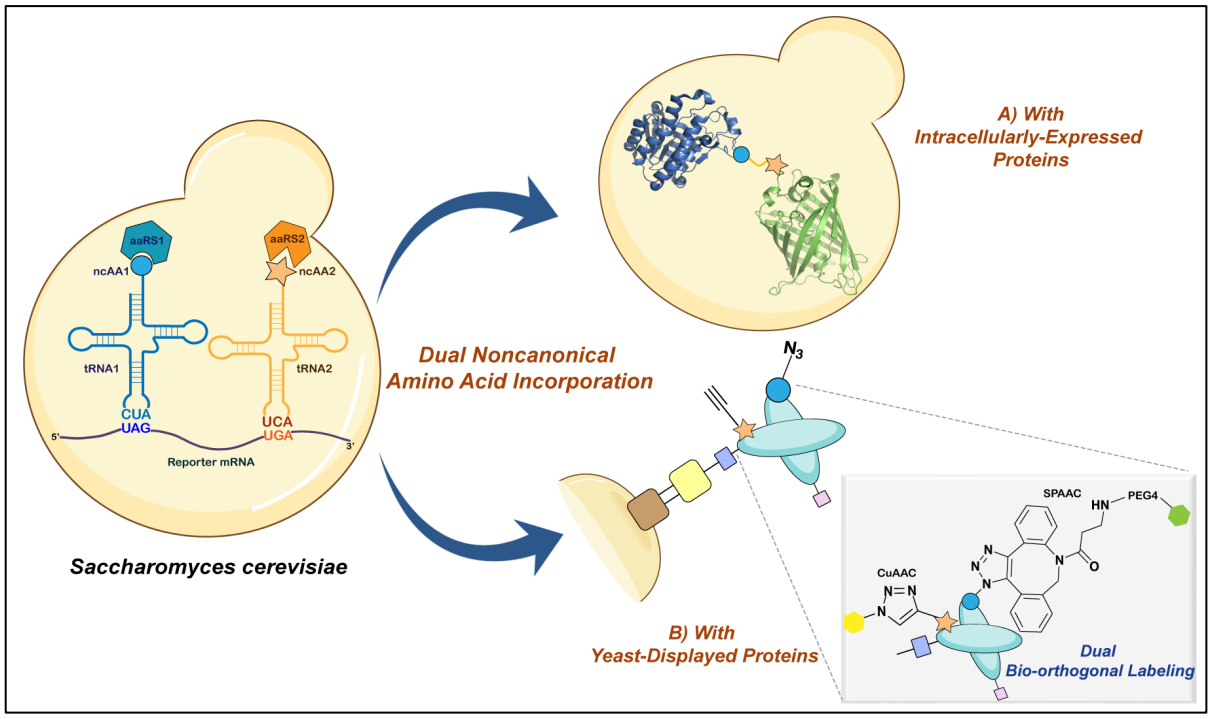

Herein we report the establishment of dual noncanonical amino acid incorporation in yeast to support expression and site-selective labelling of doubly substituted proteins in solution and on the yeast surface.

Summary:

Proteins containing noncanonical amino acids (ncAAs) provide opportunities for dissecting fundamental biological processes and engineering protein therapeutics with diverse chemistries. Incorporation of more than one ncAA into a single construct can endow a protein with multiple useful features, such as unique molecular recognition and covalent crosslinking. Herein, for the first time, we encode two chemically distinct ncAAs into proteins prepared in *Saccharomyces cerevisiae*. To complement ncAA incorporation in response to the amber (TAG) stop codon in yeast, we evaluated opal (TGA) stop codon suppression using three distinct orthogonal translation systems (OTSs): *E. coli* tyrosyl-tRNA synthetase/$tRNA^{Tyr}$, *E. coli* leucyl-tRNA synthetase/$tRNA^{Leu}$, and *M. alvus* pyrrolysyl-tRNA synthetase/$tRNA^{Pyl}$. We observed selective TGA readthrough without detectable cross-reactivity from host translation components. Further, we found that multiple factors impacted TGA readthrough efficiency in a manner analogous to TAG readthrough, including the local nucleotide context surrounding stop codons and deletion of selected genes from the yeast genome. In contrast, the identity of the suppressor tRNA affected TGA readthrough efficiency quite differently than TAG readthrough efficiency. Altogether, these observations facilitated the systematic investigation of dual ncAA incorporation in response to TAG and TGA codons within both intracellular and yeast-displayed protein constructs. Employing a proficient combination of OTSs, pairs of ncAAs could be encoded within both protein formats with efficiencies up to 6% of wildtype protein controls. Moreover, exploration of dual ncAA incorporation in yeast display format aided in demonstrating important applications of doubly-substituted proteins. First, dual ncAA incorporation within a simple synthetic antibody construct resulted in retention of antigen binding functionality, indicating that the doubly-substituted proteins can retain their basic functions. Second, presentation of reactive alkyne and azide functionalities within yeast-displayed constructs enabled sequential installation of two distinct chemical probes using bioorthogonal reactions – strain-promoted- and copper-catalyzed azide-alkyne cycloadditions (SPAAC and CuAAC) – on the yeast surface. This confirmed the ability to chemoselectively modify yeast-displayed proteins at two distinct sites. Furthermore, by utilizing a soluble form of a doubly substituted construct, we validated the feasibility to selectively double label proteins in solution in a single pot reaction. Overall, our work facilitates the addition of a 22^{nd} amino acid to the yeast genetic code and provides an important toolkit that expands the scope of applications of ncAAs for basic biological research and drug discovery in yeast.

Keywords: Noncanonical amino acids, yeast display, genetic code expansion, orthogonal translation system, Strain-promoted azide-alkyne cycloaddition, Copper(I)-catalyzed azide-alkyne cycloaddition

Introduction:

The genetic encoding of noncanonical amino acids (ncAAs) in proteins enables molecular-level manipulation of native protein structure and function as well as the introduction of new functions, properties, or chemical entities (Chin, 2014; Chung et al., 2020; Islam et al., 2021; Lewis et al., 2021; Shandell et al., 2021; Vanderschuren et al., 2022; Wang et al., 2009; Zubi et al., 2022). The number of ncAAs that can be encoded during protein biosynthesis and the number of organisms in which they can be encoded continues to expand (Dumas et al., 2015; Vargas-Rodriguez et al., 2018). The broad set of machineries now available for encoding ncAAs in proteins has led to the establishment of systems for encoding multiple, chemically distinct ncAAs in both bacterial and mammalian systems (Dunkelmann et al., 2020, 2021; Tharp et al., 2021; Zheng et al., 2018a). Dual ncAA incorporation systems have facilitated important biological applications, such as *i)* identifying mutually compatible bioconjugation chemistries for protein labeling or for monitoring protein dynamics; *ii)* aiding intra- and intermolecular protein crosslinking; and *iii)* mimicking epigenetic modifications for unravelling new protein-protein interactions (Bednar et al., 2021; Meineke et al., 2020; Sachdeva et al., 2014; Venkat et al., 2018; Wang et al., 2014; Xiao et al., 2013; Zheng et al., 2017, 2018b). However, to the best of our knowledge, such dual ncAA incorporation systems have not yet been implemented in *S. cerevisiae* or any other yeast. With reasonably fast growth kinetics and biological machinery analogous to mammalian cells, *S. cerevisiae* plays a critical role as a model organism for understanding fundamentals of eukaryotic biology as well as functions of disease-implicated genes (Botstein and Fink, 2011; Petranovic et al., 2010; Smith and Snyder, 2006). In addition, *S. cerevisiae* and other species of yeast are routinely used for large-scale production of complex recombinant proteins (Mattanovich et al., 2012). More broadly, powerful genetic, genomic, and engineering tools are available in yeast, including single-gene knockout collections, strains containing one or more synthetic chromosomes, and versatile yeast display systems (Chao et al., 2006; Cherf and Cochran, 2015; Giaever and Nislow, 2014; McMahon et al., 2018; Sanders et al., 2022). Therefore, engineering a dual ncAA incorporation system in *S. cerevisiae* would enable applications in areas of protein engineering, chemical biology, synthetic biology, and other related disciplines (Li and Liu, 2014).

The incorporation of two distinct ncAAs in cells requires the use of two orthogonal codons and two corresponding aminoacyl-tRNA-synthetase/tRNA pairs (aaRS/tRNA pairs; also referred to as orthogonal translation systems (OTSs)). These pairs must be orthogonal to one another as well as orthogonal to the host cell's native translation machinery. Together, the two OTSs drive the site-specific incorporation of two unique ncAAs in a growing polypeptide chain. Orthogonal codons can be repurposed sense codons, nonsense ("stop") codons, or engineered frameshift codons. For both bacteria and mammalian cells, orthogonal codons have been discovered and utilized in various combinations (Bednar et al., 2021; Chen et al., 2022; Hankore et al., 2019; Meineke et al., 2020; Niu et al., 2013; de la Torre and Chin, 2021; Wang et al., 2014; Willis and Chin, 2018; Zheng et al., 2017, 2018b, 2018a). However, to the best of our knowledge, in yeast only the amber (TAG) codon has been repurposed and employed for ncAA incorporation (Wiltschi, 2016). To date, the lack of additional validated orthogonal codons in yeast has hindered the development of a dual ncAA incorporation system. Another

factor slowing the progress is the absence of validated mutually-orthogonal translation systems in yeast, in contrast to a well-characterized set of mutually-orthogonal machineries available in bacteria and mammalian cells (de la Torre and Chin, 2021). These machineries were identified from an extensive repository of OTSs available in these organisms that facilitate specific and efficient decoding of multiple orthogonal codons with structurally and functionally diverse ncAAs. (Beránek et al., 2018; Biddle et al., 2022; Cervettini et al., 2020; Gan et al., 2017; Grasso et al., 2022, 2022; Italia et al., 2017; Kelemen et al., 2022; Lang et al., 2012; Wang et al., 2014; Zheng et al., 2018a).

In yeast, efforts are underway to expand the range of OTSs available for genetic code manipulation. For instance, recent reports by He *et al* and Tan *et al* demonstrated the isolation of *E. coli* aaRS variants exhibiting unique aminoacylation properties by utilizing custom selection schemes in yeast; these studies led to the identification of variants that support translation with new ncAAs including sulfotyrosine (He et al., 2020; Tan et al., 2020). Parallel efforts from our lab have led to the discovery of a broad range of *E. coli* tyrosyl-tRNA synthetase (*Ec*TyrRS) and *E. coli* Leucyl-tRNA synthetase (*Ec*LeuRS) variants with a variety of ncAA incorporation properties, including new-to-yeast ncAA incorporation and improved selectivity and activity for known ncAAs (Stieglitz and Van Deventer, 2022). In addition, work by Chatterjee and coworkers in engineered *E. coli* strains has led to the identification of additional *Ec*aaRS variants derived from *Ec*TyRS and *Ec*TrpRS with unique substrate preferences for use in mammalian cells (Grasso et al., 2022; Osgood et al., 2022). While not yet evaluated in yeast, such *Ec*aaRS variants have the potential to further broaden the range of OTSs available for use in this organism. Beyond *E. coli*-derived OTSs, translation machinery derived from archaeal Pyrrolysyl-tRNA synthetases (PylRS)-tRNA pairs continues to mature (Beránek et al., 2019; Ding et al., 2020; Dunkelmann et al., 2020; Fischer et al., 2022; Hohl et al., 2019; Meineke et al., 2018; Schmied et al., 2014; Sharma et al., 2018; Willis and Chin, 2018). PylRS-based OTSs from several organisms and their engineered derivatives support diverse ncAA incorporation and efficient decoding of a range of orthogonal codons. We and others have advanced the use of such PylRS-tRNA pairs in yeast (Hancock et al., 2010; Kleiner et al., 2013; Mukai et al., 2008; Stieglitz et al., 2022), which presents opportunities for the identification of mutually orthogonal translation systems. The growing versatility of OTSs available in yeast sets the stage for pursuing dual ncAA incorporation in this important model organism.

Herein, for the first time, we report the systematic establishment of dual ncAA incorporation systems in *S. cerevisiae* and demonstrate that these systems are suitable for applications involving both intracellular and yeast-displayed proteins. We repurpose the opal (TGA) nonsense codon to function alongside the amber (TAG) nonsense codon in yeast and demonstrate the successful decoding of these two orthogonal codons within the same mRNA transcript by different combinations of mutually orthogonal OTSs. Our detailed explorations enabled us to investigate potential non-cognate interactions that can interfere with the fidelity of the dual ncAA incorporation system and also to identify favorable genetic conditions to augment the decoding efficiencies of both TAG and TGA codons. Altogether, our dual ncAA incorporation system facilitated site-specific incorporation of different pairs of distinct ncAAs,

including ones with distinct reactive chemical handles. Furthermore, such reactive functionalities encoded in yeast-displayed constructs enabled us to generate doubly-labeled proteins by performing sequential strain-promoted azide-alkyne cycloaddition (SPAAC) and copper-catalyzed azide-alkyne cycloaddition (CuAAC) reactions directly on the yeast surface. These reactions and corroborating investigations on soluble proteins demonstrate that the two genetically-encoded, distinct chemical functionalities incorporated into proteins biosynthesized in yeast are selectively addressable.

Results:

A second orthogonal codon identified in yeast

Given the successful precedents of using the TAG codon for genetic code expansion in yeast, the most straightforward approach to access a second orthogonal codon was to repurpose another nonsense codon (Islam et al., 2021; Stieglitz et al., 2018; Wiltschi, 2016). The opal codon, TGA, is the second-least used codon next to TAG within the yeast genome, making it the preferred choice for a second codon (Trotta, 2013). Naturally occurring instances of TGA readthrough events (by near-cognate tRNAs) within yeast are known to be well-tolerated (Beznosková et al., 2019; Blanchet et al., 2014; Kohli et al., 1979; Macino et al., 1979). Moreover, TGA has been used successfully in mammalian cells for ncAA incorporation, providing further evidence for the technical feasibility of this approach (Zheng et al., 2017, 2018b). For TGA to function as an orthogonal codon in yeast, there are two important criteria to be fulfilled– *i*) Orthogonality; meaning that TGA should not be decoded at high levels by the endogenous translational machinery or non-cognate OTSs; and *ii*) Decoding efficiency; meaning that TGA should be efficiently decoded only by OTSs that utilize $tRNA_{UCA}$s and not by OTSs utilizing $tRNA_{CUA}$s or other exogenous machinery. Since there are known cases of TGA readthrough by endogenous translation machineries in yeast under selected conditions (which also holds true for TAG), the second criteria is essential to be met for minimizing aberrant readthrough (Dabrowski et al., 2015). To systematically evaluate both orthogonality and decoding efficiency at TGA codons, we used a dual-plasmid approach, where the OTS was encoded on one plasmid and the reporter protein bearing the orthogonal codon was encoded on another. This dual-plasmid approach enables the parallel assessment of different cognate and non-cognate interactions: aaRS:tRNA, aaRS:ncAA, aaRS:cAA (canonical amino acid), and codon:anticodon (Figure 1A).

We employed our previously established, galactose-inducible dual fluorescent protein reporter system to evaluate the incorporation of ncAAs in response to TGA and TAG codons (Potts et al., 2020; Stieglitz et al., 2018). In the reporter system, the N-terminal fluorescent protein (BFP) is encoded as a fusion to a C-terminal fluorescent protein (GFP) connected by a linker that contains the desired orthogonal codon. Here, the codon is positioned at a permissive site and is either TAG (referred to as BXG-TAG) or TGA (referred to as BXG-TGA) (Figure 1A). The wildtype linker sequence (TAC at the permissive site) serves as a positive control (referred to as BYG) (Potts et al., 2020) (Table S4). This dual-fluorescent reporter system enables the use of the metrics Relative Readthrough Efficiency (RRE) and Maximum Misincorporation Frequency (MMF) to evaluate characteristics of protein translation with ncAAs (Figure 1B).

RRE quantifies the readthrough of an orthogonal codon with respect to wildtype protein synthesis, with values typically ranging between 0 and 1. An RRE value of 0 indicates that all proteins produced are truncated at the orthogonal codon, while an RRE value of 1 indicates readthrough efficiency equivalent to wildtype protein synthesis. MMF reports the probability of synthesized proteins unintentionally containing a cAA at the orthogonal codon. This metric is a rigorous evaluation of ncAA incorporation fidelity because it measures the maximum possibility of cAA incorporated at an orthogonal codon. Thus, an efficient, selective ncAA incorporation at a specific site should result in a high RRE value and a corresponding low MMF value.

We utilized variants of three yeast-compatible OTSs: *E. coli* tyrosyl tRNA synthetase/$tRNA^{Tyr}$, *E. coli* leucyl tRNA synthetase/$tRNA^{Leu}$ and *M. alvus* pyrrolysyl tRNA synthetase/$tRNA^{Pyl}$ and cloned each of these OTSs separately into the pRS315 plasmid backbone under constitutive promoters (Figure 1A). Recognition of UAG or UGA codons during mRNA translation was facilitated by mutating the anticodon sequences of suppressor tRNAs to CUA or UCA, respectively. This simple approach allowed for evaluation of cognate and non-cognate aminoacylation events to determine whether the aaRSs used can tolerate changes in anticodons, as anticodon identity is known to modulate tRNA recognition and aminoacylation in many aaRSs (Reynolds et al., 2017). For the *Ec*LeuRS/$tRNA^{Leu}$ pair, we used the polyspecific aaRS variant LeuOmeRS with a T252A mutation in its editing domain and employed the ncAA *O*-methyl-L-tyrosine (**1**; OmeY) as a substrate (Wu et al., 2004). For the *Ec*TyrRS/$tRNA^{Tyr}$ pair, we employed a polyspecific aaRS variant, T2RS5, identified through our high-throughput screening and used it with the ncAA *p*-propargyloxyl-L-phenylalanine (**2**; OPG) as a substrate (Stieglitz and Van Deventer, 2022). Lastly, for the PylRS/$tRNA^{Pyl}$ pair, we used the *M. alvus* PylRS with the ncAA N^{ε}-Boc-L-Lysine (**3**; BocK) as a substrate (Stieglitz et al., 2022) (Figure 1C).

For our initial investigation of ncAA incorporation at TGA codons, we conducted a series of flow cytometry experiments to determine RRE and MMF at "cognate" and "noncognate" orthogonal codons for each of the OTSs (Figure 1D). The three aaRS-tRNA pairs encoding plasmids with either $tRNA_{CUA}$ or $tRNA_{UCA}$ were separately co-transformed into the *S. cerevisiae* strain RJY100 with a reporter construct encoding a cognate or a non-cognate orthogonal codon, or a WT reporter (absence of orthogonal codons; Figure 1A) (Van Deventer et al., 2015, 2016). All transformants were induced either in the absence or in the presence of 1 mM cognate ncAA and subjected to flow cytometry analysis and RRE and MMF calculations (Figure 1A; Figure S1). Notably, all three OTSs supported ncAA incorporation in response to TGA when the OTSs contained tRNAs with the corresponding UCA anticodon, but not a noncognate anticodon. Additionally, quantitative analyses indicated high RRE and low MMF values for all cognate OTS:reporter combinations tested, and the opposite trend for non-cognate OTS:reporter combinations. These data demonstrate that these OTSs exhibit specificity at the codon:anticodon interaction level, without any detectable cross-reactivity (Figure 1C and 1D). Moreover, both flow cytometry dot plots and median fluorescence intensity (MFI) graphs indicate background levels of fluorescence in the absence of any ncAAs for both TAG and TGA codons, suggesting negligible participation of endogenous translation

machinery in codon readthrough events (Figure S1 and S2). In comparison with TAG, TGA was decoded 2-6 fold less efficiently by both T2RS5/$tRNA_{UCA}^{Tyr}$ and LeuOmeRS/$tRNA_{UCA}^{Leu}$ pairs (Figure 1C). A lower level of TGA readthrough by the two *E. coli* OTSs, in comparison to TAG readthrough, is not without precedent. Previous studies from Chatterjee and coworkers in mammalian cells reported similar trends (Zheng et al., 2017). In contrast, for the *Ma*PylRS/$tRNA^{Pyl}$ pair, the decoding efficiencies of both TAG and TGA codons were determined to be at equivalent levels when paired with tRNAs containing the "cognate" anticodon (Figure 1C). Consistent with our prior work, we observed low RRE values for *Ma*PylRS systems, which are poorly distinguishable from control samples (Stieglitz et al., 2022). Hence, to further corroborate the translational activities of these samples, we evaluated MFIs of C-terminal reporter expression and observed clear differences in fluorescence between samples induced in the absence and presence of ncAAs (Figure S2). Overall, these data establish TGA as an orthogonal codon in yeast for site-specific ncAA incorporation, with no detectable cross-reactivity with TAG at the codon:anticodon level.

Sequence context impacts TGA suppression efficiency

Prior to combining constructs encoding both TAG and TGA codons for dual ncAA incorporation, we sought to better understand underlying factors that can influence ncAA incorporation in response to TGA. One factor known to govern variations in readthrough efficiencies is the local sequence context surrounding an orthogonal codon. A few recent studies have reported that nucleotides upstream and downstream of TAG codons can impact ncAA incorporation efficiency in both bacteria and mammalian expression systems (Bartoschek et al., 2021; Chen et al., 2022; Pott et al., 2014; Xu et al., 2016). Likewise, past studies from Cornish and coworkers and from our own group have confirmed the nucleotide context dependency on TAG codon readthrough efficiency in yeast (Anzalone et al., 2019; Potts et al., 2020). Therefore, based on these observations and the fact that natural TGA readthrough events in yeast by near-cognate tRNAs (with a cAA) are dictated by their neighboring nucleotides, we sought to investigate ncAA incorporation efficiency in response to TGA codons positioned at alternate locations within the linker of our dual-fluorescent reporter system (Beznosková et al., 2016, 2019; McCaughan et al., 1995). For our experimental purpose, we selected the position within the 'Alt-TAG' reporter construct, first described in our prior work, as it demonstrated moderate but significantly decreased readthrough across different OTS and ncAA combinations (Potts et al., 2020). Here, we were interested in understanding whether the same trend would hold when TAG was replaced with TGA in this construct (Figure 1A, Table S4). To quantify solely the changes related to orthogonal codon position, experimental parameters including OTS identities, induction conditions, and ncAA types were all kept identical to the experimental parameters used in combination with BXG reporters.

To our satisfaction, flow-cytometric analysis revealed similar ncAA incorporation efficiency and fidelity trends at the alternate TGA (Alt-TGA) position as at the BXG-TGA position, irrespective of the OTS used (Figure 2A, S3, and S4A). For both *E. coli* OTSs, ncAA incorporation in response to TAG was more efficient than incorporation in response to TGA, while for the *Ma*PylRS/$tRNA^{Pyl}$ OTS, ncAA incorporation in response to either TAG or TGA

(with corresponding "cognate" tRNAs) was comparable; this is evident in evaluations of RRE, MMF, and median fluorescence intensities of C-terminal GFP fluorescence levels (Figure 2A and S4). Interestingly, comparing RRE values between the two stop codon positions (BXG- v/s Alt- reporters) confirmed that the overall readthrough at the alternate, N-terminal stop codon position (within the Alt- construct) was substantially lower than the corresponding readthrough at the C-terminal codon position (within the BXG- construct). This corroborated our previous findings that the nucleotide environment around the orthogonal codon impacts the readthrough efficiency in yeast, and suggests that this trend holds irrespective of whether the readthrough occurs at a TAG or TGA codon (Potts et al., 2020). To further assess changes in readthrough performance that occur between the two stop codon positions, we determined the ratios of the MFIs of GFP fluorescence for cognate OTS:reporter combinations at the BXG or BXG-TGA position to the Alt-TAG or Alt-TGA position (Figure 2B). Surprisingly, when comparing changes in readthrough at these two positions, the resulting fold changes in TGA readthrough across the three OTSs was distinct in comparison to corresponding fold changes in TAG. Theoretically, the fold change for a particular nonsense codon should not change between OTSs if the nucleotide context of the reporter is the sole contributing factor to readthrough efficiency. We attribute the observed additional changes in TGA readthrough (in comparison to TAG readthrough) to the anticodon change in the tRNA and to differences in the nucleotide sequences (and presumably identity elements) of the tRNAs in each OTS. Therefore, it can be concluded that efficient codon:anticodon interactions are governed by specific features of both the stop codon sequence context in the reporter and the nucleotide sequence of the tRNA component of the OTS.

Single-gene knockout yeast strains enhance readthrough efficiency

Numerous engineering strategies are known to augment stop codon readthrough, including single-gene deletions, whole-genome synthesis, and engineering various components of the translation machinery (DeBenedictis et al., 2021; Dunkelmann et al., 2021; Gan et al., 2017; Sanders et al., 2022; Stieglitz and Van Deventer, 2022; de la Torre and Chin, 2021; Zackin et al., 2022). Prior work from our group has shown that the use of single-gene knockout strains of *S. cerevisiae* can enhance ncAA incorporation efficiencies in response to the TAG codon for a range of OTSs and ncAAs (Potts et al., 2020; Stieglitz et al., 2021; Zackin et al., 2022). Here, we sought to investigate whether the relatively poor ncAA incorporation efficiencies we observed in response to TGA could be improved by use of single-gene deletion strains. We focused our investigations on deletion of *TPA1* and *PPQ1*. Elimination of these genes was previously found to enhance nonsense suppression with near-cognate tRNAs and, in our past work, these eliminations enhanced ncAA incorporation in response to TAG for multiple OTSs and ncAAs (von der Haar and Tuite, 2007; Potts et al., 2020; Stieglitz et al., 2021). *TPA1* is associated with a deadenylase complex that regulates mRNA poly(A) tail length and interacts with eukaryotic release factors eRF1 and eRF3 (Keeling et al., 2006). On the other hand, the gene product of *PPQ1* is a serine/threonine phosphatase with a still-undefined role in the termination of translation (Song and Liebman, 1987). We conducted analyses with knockouts within the BY4741 strain background since the relevant single-gene deletion strains were readily available. This necessitated transferring the BXG- and Alt- reporter constructs from a pCTCON2-plasmid backbone (*TRP1* marker) to a pRS416-plasmid backbone (*URA3* marker),

since *trp1* is not an available auxotrophic marker in BY4741. Otherwise, the conditions used for exploring the effects of single-gene deletions on ncAA incorporation efficiency in response to TGA were identical to the conditions used for our initial investigations in the RJY100 strain. TAG-containing reporter constructs were included for side-by-side comparison of readthrough effects in *ppq1Δ* and *tpa1Δ* strains.

Evaluations of ncAA incorporation efficiency were conducted via flow cytometry for all strains using each of the 3 OTSs and 2 stop codon positions summarized in Figure 1A. Analysis of RRE revealed 2-3 fold enhancements in TGA readthrough across different OTSs and codon positions with the *ppq1Δ* strain relative to the WT BY4741 strain. Improvements were more apparent for the Alt-TGA (and Alt-TAG) constructs than for the corresponding BXG constructs (Figure 3; Figure S5-S7). On other hand, for the *tpa1Δ* strain, slight increases in readthrough efficiency were only observed in some cases where *Ec*TyrRS/tRNA^{Tyr} or *Ec*LeuRS/tRNA^{Leu} OTSs were used. In the case of *Ma*PylRS/tRNA^{Pyl}, no enhancements in TGA readthrough efficiencies were observed in *tpa1Δ* under the conditions tested. Under all conditions tested here, improvements in ncAA incorporation efficiency in knockout strains were not accompanied by detectable changes to the apparent fidelity of ncAA incorporation, as evidenced by the lack of changes in MMF (Figure S8-S9). The overall trends in RRE values determined in BY4741 strains were consistent with the trends observed in RJY100; most notably, RRE values for ncAA incorporation at TGA codons were lower than RRE values at TAG codons under corresponding conditions (Figure 1D and 3A; Figure 2A and 3B). Interestingly, when changing the plasmid backbone from pCTCON2 to pRS416, there was a modest decrease in RRE values with LeuOmeRS/tRNA^{Leu} OTSs for both TAG and TGA, but not for the other two OTSs. These observations are consistent with our previous results, indicating that changes in plasmid backbone can impact the apparent performance of some OTSs for reasons that have not yet been elucidated (Potts et al., 2020). In summary, the *ppq1Δ* strain enhanced ncAA incorporation across both orthogonal codons, independent of the codon position or OTS type.

Dual ncAA incorporation system for intracellular proteins

With a broad understanding of factors that influence ncAA incorporation at both TAG and TGA sites in separate constructs, we next sought to utilize two OTSs in the same host cell to enable dual ncAA incorporation within a single protein. For facilitating expression of two OTSs, we replaced the reporter plasmid with our previously described single plasmid system encoding both a TAG-suppressing OTS and the inducible reporter system (Stieglitz et al., 2021) (Figure 4A). The reporter encoded within the single plasmid system was further modified to encode both TAG and TGA in the linker at the "BXG" and "Alt" positions in both possible orientations, leading to generation of two mutant reporters: BX$_2$G-AO (A: Amber (TAG); O: Opal (TGA)) and BX$_2$G-OA. These plasmids were co-transformed with a separate plasmid encoding the second, TGA-suppressing OTS. We used a single-plasmid version of the BYG reporter (orthogonal codons absent) as a positive control and to facilitate RRE and MMF calculations (Figure 4A). For these initial analyses of dual ncAA incorporation, we selected the *Ec*TyrRS/tRNA^{Tyr} pair to suppress the TAG codon because it exhibited the highest TAG

codon readthrough in the BY4741 background among all the OTSs and across different codon positions. We employed the TyrOmeRS variant in place of the T2RS5 variant because TyrOmeRS exhibits narrower ncAA substrate preferences than T2RS5 (Chin, 2003). We used the same OTS variants to suppress TGA as were used in the investigations above, resulting in the following combinations of OTSs for dual ncAA incorporation experiments: *Ec*TyrRS(TyrOmeRS)/$tRNA_{CUA}^{Tyr}$ + *Ec*LeuRS(LeuOmeRS)/$tRNA_{UCA}^{Leu}$ (hereafter, referred as '$TyrRS_{TAG}$ + $LeuRS_{TGA}$') and *Ec*TyrRS(TyrOmeRS)/$tRNA_{CUA}^{Tyr}$ + *Ma*PylRS/$tRNA_{UCA}^{Pyl}$ (hereafter, referred as '$TyrRS_{TAG}$ + $PylRS_{TGA}$') (Figure 4A). For both BY4741 and *ppq1Δ* strains, we induced cells under three sets of conditions: *i)* absence of ncAAs; *ii)* presence of one ncAA; and *iii)* presence of both ncAAs. These sets of conditions allowed systematic evaluation of cognate readthrough events as well as identification of aberrant readthrough events that may result from non-cognate interactions such as aaRSs:tRNA or aaRSs:ncAA (Figure 4A). To minimize the potential for off-target aaRS:ncAA interactions, the ncAAs recognized most efficiently by their "cognate" OTSs were selected: 4-Azidomethyl-L-phenylalanine (**6**) as a substrate for LeuOmeRS, 4-Azido-L-phenylalanine (**4**) for TyrOmeRS and, N^{ε}-Boc-L-Lysine (**5**) for MaPylRS.

Following induction under all conditions, we conducted flow cytometry to explore dual ncAA incorporation. Satisfyingly, both dot plots and RRE calculations revealed clear evidence of full-length reporter expression in the presence of both ncAAs, for both OTS combinations and both orientations of orthogonal codon positions, (BX_2G-AO or BX_2G-OA) (Figure 4B-E, Figure S10-S11). Quantitatively, the amount of full-length reporter detected was 1–6% of wild-type reporter expression levels (Figure 4C and 4E). As expected, readthrough efficiency in *ppq1Δ* was higher than in BY4741, improving RRE for the $TyrRS_{TAG}$ + $LeuRS_{TGA}$ combination by 3–6 fold, while the RRE for the $TyrRS_{TAG}$ + $PylRS_{TGA}$ combination was improved by 2–3 fold (Figure 4C and 4E). Readthrough levels remained at background levels in the absence of ncAAs, but low levels of full-length reporter expression (<1% of the BYG WT control reporter) were observed when cells were induced in the presence of a single ncAA. These aberrant readthrough events were more pronounced with the $TyrRS_{TAG}$ + $LeuRS_{TGA}$ combination of OTSs, likely due to non-cognate aaRSs:tRNA or aaRSs:ncAA interactions (Figure 4B-C). This observation is in line with prior work from Zheng *et al* in mammalian cells, where it was demonstrated that mutating the *E. coli* tRNA anticodon sequence resulted in recognition by non-cognate *E. coli* aaRSs (Zheng et al., 2017). In addition, since AzF and AzMF only differ by a methylene unit, there is a possibility of either of the aaRSs recognizing the "non-cognate" but structurally related ncAA. There is some evidence for low-level AzF incorporation by LeuOmeRS in our earlier work (Potts et al., 2020; Stieglitz et al., 2018). In comparison to $TyrRS_{TAG}$ + $LeuRS_{TGA}$, the $TyrRS_{TAG}$ + $PylRS_{TGA}$ OTS combination exhibited much lower RRE values for both orientations of stop codons. This is consistent both with our above results and with our prior work (Figure 3) (Stieglitz et al., 2022). Readthrough efficiencies were also affected by the orientation of the two orthogonal codons within the reporter. Readthrough experiments with BX_2G-AO led to approximately 4-fold higher levels of full-length reporter than experiments with BX_2G-OA for both of the OTS combinations evaluated here. These results are in agreement with our observations of individual TAG and TGA codon readthrough

events at BXG- and Alt- stop codon positions. As highlighted in Figure 2A and C, the BXG position is more permissive for orthogonal codon readthrough than the Alt position. As TGA is decoded at lower levels than TAG by the OTSs used here, having TGA at a more permissive position (BX_2G-AO rather than BX_2G-OA) facilitated higher overall readthrough (Figure 4C and E). In conclusion, these experiments demonstrate the feasibility of conducting dual ncAA incorporation in yeast, with the combination of $TyrRS_{TAG}$ + $LeuRS_{TGA}$ yielding up to 6% of wild-type reporter levels.

Dual ncAA incorporation system established in yeast display format

We next sought to extend our dual ncAA incorporation system to yeast-displayed proteins. Yeast display serves as a powerful platform to engineer proteins and enzymes and supports assays for quantitatively evaluating protein properties including affinity, stability, activity, and specificity (Cherf and Cochran, 2015). Previously, we have shown that chemically expanding yeast-displayed antibodies with ncAAs results in constructs with new properties including bio-orthogonal reactivity, photocrosslinkability, and spontaneous crosslinkability (Alcala-Torano et al., 2022; Islam et al., 2021). Incorporation of a second noncanonical functionality within chemically expanded, yeast-displayed proteins is expected to usher in a broader range of applications such as the preparation of doubly labeled proteins, parallel introduction of two distinct chemical properties such as crosslinkable groups and recognition motifs (for example, post-translational modifications), or additional chemical moieties of fundamental importance or commercial value (Oller-Salvia and Chin, 2019; Zheng et al., 2018b).

Herein, we explored the feasibility of dual ncAA incorporation on the yeast surface by encoding sites for the incorporation of two distinct ncAAs into a previously reported synthetic antibody fragment (Donkey1.1 scFv) known to tolerate ncAA incorporation at several substitution sites (Figure 5A) (Islam et al., 2021). We chose the positions L93 (located in complementarity determining region L3; CDR-L3) and H54 (located in CDR-H2) for encoding ncAAs in response to TAG and TGA. The two codons were incorporated interchangeably at both of the sites, giving rise to two reporter constructs: Donkey1.1-AO and Donkey1.1-OA (Figure 5A; the nomenclature for AO and OA is the same as stated in the previous section). N- and C-terminal epitope tags (HA and c-myc) were utilized for quantitative flow cytometric evaluation of protein display levels. A wild-type version of the reporter protein was used as a control and to facilitate calculation of RRE and MMF. Similarly to the set of plasmids used for the intracellular dual ncAA incorporation system, a TAG-suppressing OTS was cloned upstream of the reporter in the pCTCON2 vector backbone to generate a single-plasmid yeast display + ncAA incorporation system. The TGA-suppressing OTS was cloned separately into the pRS315 vector backbone, and subsequently, both plasmids were transformed into the yeast display strain RJY100 (Van Deventer et al., 2015). This Aga1p-Aga2p-based display system facilitates the use of induction procedures identical to those used for dual fluorescent reporters. For preparation of a "mutually orthogonal" *Ec*TyrRS/$tRNA_{CUA}^{Tyr}$ + *Ec*LeuRS/$tRNA_{UCA}^{Leu}$ combination, we used the TyrAcFRS variant as part of an *Ec*TyrRS/$tRNA_{CUA}^{Tyr}$ OTS to suppress TAG, and a newly-identified variant termed LysAlkRS3 as part of the *Ec*LeuRS/$tRNA_{UCA}^{Leu}$ OTS to suppress TGA (Stieglitz and Van Deventer, 2022). These OTSs were chosen based on their nonoverlapping substrate specificities, where the ncAA AzF (**4**)

can be encoded with TyrAcFRS/$tRNA_{CUA}^{Tyr}$, and the ncAA LysAlk (**5**) can be encoded with LysAlkRS3/$tRNA_{UCA}^{Leu}$. The purpose of choosing ncAAs with bio-orthogonal reactive handles in these experiments was to facilitate investigations of double labeling strategies on the yeast surface.

We conducted flow cytometry experiments analogous to those used for the intracellular reporters to evaluate dual ncAA incorporation efficiency and fidelity. Flow cytometry dot plots revealed the presence of doubly-positive populations (HA+ and c-myc+) for both stop codon orientations following induction in the presence of AzF and LysAlk, providing tangible evidence of full-length protein display on the yeast surface (Figure 5B). RRE analysis indicated that the full-length antibody display ranged between 1–4% of WT protein display levels. As observed with intracellular reporters, low levels of full-length protein (<1% of the WT protein) were also detected following induction in the presence of a single ncAA. This signal was most apparent when cultures were induced in the presence of AzF, and could be the result of non-cognate interactions between TyrAcFRS and $tRNA^{Leu}$; LysAlkRS3 and AzF; or LysAlkRS3 and canonical amino acids (Stieglitz and Van Deventer, 2022). A comparison of full-length protein display levels revealed that the orientation of the orthogonal codons within the Donkey1.1-OA construct leads to 3.5-fold higher full-length protein than the orientation of the orthogonal codons within the Donkey1.1-AO construct. This implies that the L93 position is more permissive for TGA readthrough than H54, consistent with our prior observation with TAG readthrough events (Figure 5C) (Islam et al., 2021).

We also evaluated whether the binding functionalities of doubly substituted clones were retained. Donkey1.1 (and other simple synthetic antibodies) mediate antigen recognition predominantly through CDR-H3 and exhibit tolerance for single ncAA substitutions at several locations distal to CDR-H3 (Islam et al., 2021). To assess the binding function in doubly substituted clones, we conducted yeast surface titration experiments with both displayed antibody reporters to determine antigen binding levels and estimate K_D values. A wild-type version of the reporter, which does not contain any ncAAs, was included as a positive control. For both doubly substituted clones, we observed clear antigen binding for concentrations as low as 3.3 nM (Figure 5D and S14). However, these assays also revealed that the apparent binding affinities were decreased by roughly 2 orders of magnitude in comparison to the WT protein (K_{Dapp}: 9.1 nM); for both Donkey1.1- OA and Donkey1.1-AO, apparent K_Ds were estimated to be in range of approximately 3–5 μM. Given that we previously observed some loss of binding affinity upon single ncAA substitution at both L93 and H54, it seems reasonable to observe further loss of binding affinity upon the introduction of a second ncAA within the same construct. Another possibility is that the low display levels of doubly substituted constructs, which result in reduced avidity on the yeast surface, decrease the apparent affinities of the constructs for the dimeric IgG antigen. Nevertheless, these data clearly demonstrate the feasibility of performing dual ncAA incorporation on the yeast surface, and further provide evidence for the retention of antigen binding functionality in doubly substituted synthetic antibody variants.

Chemoselective double labeling of yeast-displayed and soluble proteins

Covalent attachment of two distinct chemical probes to dual ncAA-substituted proteins has enabled diverse biological applications, including FRET for studying protein conformation and dynamics (Bednar et al., 2021; Meineke et al., 2020; Wang et al., 2014). Here, we investigate, for what we believe is the first time, the combination of SPAAC and CuAAC reactions to install two different chemical probes within yeast-displayed proteins. Generally, SPAAC and CuAAC reactions are not considered mutually compatible, as they both require azide reactants. However, prior studies have demonstrated that sequential use of SPAAC and CuAAC reactions can support selective biomolecule labeling, both *in vivo* and *in vitro* (Holstein et al., 2017; Lion et al., 2017; Simon et al., 2018; Truong et al., 2012; Winz et al., 2018). For facilitating exploration of such sequential reactions with our system, we used the yeast-displayed dual ncAA-containing antibody reporters Donkey1.1-AO and Donkey1.1-OA (Figure 5A; see previous section) along with the corresponding wild-type control. Figure 6A outlines the reaction conditions and probes used for labeling. Consistent with previous studies, it was essential to perform SPAAC on the azide present in the displayed protein of interest before conducting CuAAC to ensure that all free azides were consumed prior to exogenous addition of an azide probe for CuAAC. Flow cytometry analysis was used to evaluate all SPAAC and CuAAC reactions performed on doubly substituted proteins displayed on the yeast surface.

We first examined each reaction individually with both Donkey1.1-OA and Donkey1.1-AO constructs to identify efficient reaction conditions. Flow cytometry data from single-labeling studies with SPAAC and CuAAC reactions revealed double-positive populations for Donkey1.1-OA signifying that the full-length OA construct (c-myc+) had successfully undergone either SPAAC (biotin+) or CuAAC (Alexa Fluor 405+) reactions (Figure S15). On other hand, for the Donkey1.1-AO reporter protein, the flow cytometry data provided clear evidence for SPAAC, but not for CuAAC reactions, where high background fluorescence was observed. This made it difficult to delineate specific CuAAC labeling (Alexa Fluor 405+) of full-length proteins (c-myc+) from non-specific labeling of yeast cells (Figure S15). We attribute the lack of specific signal to low levels of LysAlk (**5**) at the H54 site, which is observed to be a less permissive site for TGA suppression. Thus, we proceeded on performing sequential, double labeling with the Donkey1.1-OA construct as it unambiguously supported selective bioorthogonal reactions (SPAAC and CuAAC) (Figure 6A). Dot plots indicated elevated detection levels of both biotin (SPAAC) and Alexa Fluor 405 (CuAAC) probes in c-myc+ populations of Donkey1.1-OA samples. Such signals were undetected in the case of c-myc– cells of Donkey1.1-OA or in any cells of Donkey1.1-WT samples (Figure 6B, left panel). Additionally, dot plots of biotin detection versus Alexa Fluor 405 detection confirmed that both the SPAAC and CuAAC probes were present on the same population of Donkey1.1-OA cells (Figure 6B, right panels). Quantitative evaluation of the c-myc+ populations for the SPAAC (biotin) and CuAAC (Alexa Fluor 405) probes further substantiated the statistically significant increments in the fluorescent signal of Donkey1.1-OA samples in comparison to Donkey1.1-WT samples (Figure 6C). All these data provide direct evidence of double-labeling of yeast-displayed proteins and confirm that both azide and alkyne functionalities encoded within the Donkey1.1-OA antibody construct can be selectively addressed using sequential SPAAC and CuAAC reactions.

To further validate the observations in yeast display format, we investigated the reactivities of soluble forms of Donkey1.1-OA and Donkey1.1-WT. Using plasmids encoding secreted scFv-Fc constructs, we prepared and isolated pure forms of each protein via protein A affinity chromatography as determined by SDS-PAGE (Figure 6D; Figure S16) (Hershman et al., 2022; Islam et al., 2021). We attempted matrix-assisted laser desorption ionization (MALDI) mass spectrometry to corroborate the incorporation of the two distinct ncAAs within the purified Donkey1.1-OA reporter. Analysis of trypsinized samples resulted in the detection of the peptide peak corresponding to the H54 fragment, which harbors AzF (**4**) (Figure S17). As we and others have previously observed, we detected a loss of 28 mass units (m/z – 2309 Da) compared to the expected mass (m/z – 2335 Da), which corresponds to azide decomposition during MALDI (via N_2 removal) (Li et al., 2010; Stieglitz and Van Deventer, 2022). However, the peak corresponding to the L93 peptide fragment could not be detected, which we attribute to its large size (m/z – 4554 Da). Low sample yields and complex glycosylation patterns precluded the use of alternative mass spectrometric methods for analysis. Therefore, we focused on probing the SPAAC and CuAAC reactivities of Donkey1.1-OA in soluble scFv format via SDS-PAGE and Western blotting. With individual SPAAC (probe: DBCO-PEG4-biotin) and CuAAC reactions (probe: picolyl azide Alexa Fluor 647) in solution, we detected protein labeling only with Donkey1.1-OA and not with the Donkey1.1-WT control (Figure 6D). This data clearly confirmed the presence of two noncanonical functionalities in Donkey1.1-OA and confirmed the selectivity of individual SPAAC and CuAAC reactions in solution. Finally, utilizing the identified reaction conditions, we explored double labeling of Donkey1.1-OA in a single pot reaction (Figure 6D). Clear signals for both probes were evident in the Donkey1.1-OA sample, subjected to the sequential bioorthogonal reactions. To achieve these signals, we treated samples with low concentrations of the SPAAC probe for extended reaction times to attempt to minimize interference of unreacted DBCO with the CuAAC probe (picolyl azide Alexa Fluor 647). Despite these efforts, a small amount of non-specific background reaction did occur, as suggested by the lower intensity of the biotin detection of the doubly labeled Donkey1.1-OA in comparison to the detection of the sample treated only with the SPAAC probe (Figure 6D, biotin detection panel). Overall, for the first time, we have successfully demonstrated the feasibility of performing two distinct conjugations on yeast-prepared, doubly substituted proteins in both yeast display format and on secreted, purified proteins.

Discussion

In this study, we have identified and systematically characterized orthogonal translation systems, gene deletions, and stop codon contexts that support (and enhance) the incorporation of diverse ncAAs in response to opal (TGA) codons in yeast. Combining these systems with mutually orthogonal amber suppression machineries, we established dual ncAA incorporation in yeast for the first time with both soluble and yeast-displayed proteins. In both formats, we could exploit the encoded ncAAs for biorthogonal conjugation reactions to achieve double labeling, demonstrating the utility of our engineered system for presenting multiple, distinct functionalities within a single protein.

In our initial investigations of ncAA incorporation in response to TGA, we determined that variants from three distinct classes of OTSs in yeast – *Ec*TyrRS/tRNA^{Tyr}, *Ec*LeuRS/tRNA^{Leu} and *Ma*PylRS/tRNA^{Pyl} – supported significant ncAA incorporation without any detectable readthrough from either orthogonal tRNA$_{CUA}$s or from endogenous aaRS-tRNA pairs. Such versatile decoding of TGA allowed us to identify two different OTS combinations that support dual ncAA incorporation in yeast: TyrRS/tRNA$_{CUA}$^{Tyr} + LeuRS/tRNA$_{UCA}$^{Leu} and TyrRS/tRNA$_{CUA}$^{Tyr} + PylRS/tRNA$_{UCA}$^{Pyl}. Both combinations facilitated incorporation of two distinct ncAAs in proteins expressed intracellularly, and the TyrRS/tRNA$_{CUA}$^{Tyr} + LeuRS/tRNA$_{UCA}$^{Leu} combination further facilitated dual ncAA incorporation in yeast display format. However, we did observe some evidence for aberrant production of full-length protein when the dual incorporation systems were induced in the presence of only a single ncAA (most notably with TyrRS/tRNA$_{CUA}$^{Tyr} + LeuRS/tRNA$_{UCA}$^{Leu}). This may be attributable to one or more of the following: 1) mischarging of tRNA by non-cognate aaRSs (for example, tRNA$_{CUA}$^{Tyr} by LeuRS); 2) recognition of a non-cognate amino acid substrate by an aaRS (for example, TyrRS recognizing AzMF, instead of its "cognate" AzF substrate); or 3) mischarging of a tRNA with a cAA (for example, tRNA$_{CUA}$^{Tyr} is charged with tryptophan rather than the ncAA of interest). The first possibility is a known phenomenon observed by Chatterjee and coworkers when using a combination of *E. coli* aaRSs in mammalian cells (Zheng et al., 2017). Mutating the anticodon sequence of a tRNA can result in the tRNA becoming a substrate of a non-cognate *E. coli* aaRS. In the future, such crosstalk could be mitigated by engineering or designing tRNAs to reduce such phenomena. The second possibility (noncognate ncAA charging) arises due to the polyspecific nature of many engineered aaRSs (Stieglitz et al., 2018). This challenge could be avoided by utilizing aaRSs with non-overlapping sets of substrates. High-throughput engineering efforts from our lab and others have demonstrated the possibility of engineering highly specific aaRSs that discriminate against closely related ncAA substrates (Amiram et al., 2015; Meineke et al., 2020; Stieglitz and Van Deventer, 2022; Willis and Chin, 2018). Lastly, the third possibility (canonical amino acid mischarging) is a known challenge associated with engineering aaRSs for genetic code expansion (Amiram et al., 2015; Italia et al., 2018; Jones et al., 2021; Kunjapur et al., 2018; Stieglitz and Van Deventer, 2022). While a portion of this challenge can be mitigated by using high ncAA concentrations during induction of protein synthesis, the discovery of additional high-performing aaRS variants that discriminate against the canonical amino acids will be important going forward. Dual ncAA incorporation in yeast will certainly benefit from ongoing efforts to expand the availability and performance of OTSs to access a broader palette of genetically encodable ncAAs with useful chemistries (Dunkelmann et al., 2020; Grasso et al., 2022; He et al., 2020; Italia et al., 2017; Osgood et al., 2022; Stieglitz and Van Deventer, 2021; Tan et al., 2020).

Identification of mutually orthogonal pairs of OTSs in yeast enabled us to prepare doubly substituted synthetic antibodies with distinctive reactive functionalities. These constructs retained their binding function, albeit with some loss of affinity, and facilitated efficient labeling with two distinct bioorthogonal chemistries. Sequential SPAAC and CuAAC reactions led to doubly functionalized antibodies in both yeast display and soluble formats, which to the best of our knowledge has not previously been achieved in yeast-based ncAA incorporation systems. Other bioorthogonal conjugation reactions that are promising candidates for double

labeling on the yeast surface and in yeast-produced proteins include reactions such as strain-promoted inverse electron-demand Diels-Alder cycloaddition (SPIEDAC) and chemoselective rapid azo-coupling reaction (CRACR) (Bednar et al., 2021; Italia et al., 2019; Meineke et al., 2020; Oller-Salvia and Chin, 2019; Row and Prescher, 2018; Zheng et al., 2017, 2018a). Efficient routes to doubly labeled proteins on the yeast surface are expected to enable applications such as FRET to study protein conformation and dynamics; doubly labeled proteins have previously facilitated FRET studies *in vitro* and *in vivo*, including on the surfaces of live mammalian cells (Cui et al., 2017; Maurel et al., 2008; Wang et al., 2014; Wu et al., 2012). Beyond bioconjugation strategies, proteins with dual ncAAs can support applications including intramolecular protein stapling, tethering strategies for small molecules or other drug modalities, and simultaneous presentation of two distinct chemistries such as crosslinking chemistries and posttranslational modifications (Alcala-Torano et al., 2022; Bednar et al., 2021; Islam et al., 2021; Meineke et al., 2020; Ren et al.; Zheng et al., 2018b). Thus, the emerging dual ncAA incorporation strategies in this work along with the expanding collection of OTSs supporting diverse ncAA incorporation in yeast will streamline the realization of these intricate protein manipulations in the near future.

Despite the successful implementation of dual ncAA incorporation in yeast, the systems described here exhibit relatively low efficiencies. A major limiting factor is the lower readthrough efficiency of TGA compared to TAG by the *E. coli* OTSs used here. One likely explanation is that the anticodon change from CUA to UCA is not well-tolerated in the tRNAs. The changes in readthrough efficiency we observe in going from amber to opal codon suppression appear to be tRNA-dependent, suggesting that poor recognition of tRNA identity elements plays a role in determining TGA decoding efficiency. Anticodon mutations may interfere with tRNA recognition by cognate *E. coli* aaRSs (Reynolds et al., 2017). In addition, these mutations may interfere with the biochemical installation of post-transcriptional modifications. These modifications, which are frequently dictated by anticodon sequence, are responsible for stabilizing codon-anticodon interactions (Uhlenbeck and Schrader, 2018) and may be absent in the engineered systems used in this study. Inefficiencies from poor tRNA recognition can be alleviated either by enhancing the expression levels of these tRNAs to increase tRNA abundance, or by engineering suppressor tRNAs that improve tRNA recognition. Several recent studies have identified mutant tRNAs that enhance ncAA incorporation efficiencies, confirming the feasibility of pursuing tRNA engineering strategies (DeBenedictis et al., 2021; Fan et al., 2015; Guo et al., 2009; Kelemen et al., 2022). In addition to tRNA properties, our data indicate that the nucleotide context surrounding opal codons also plays a role in dictating ncAA incorporation efficiency. The effects of changing the context around an opal codon appear to be similar to the effects of changing the context around an amber codon. This is consistent with prior work from our own group and work from other groups investigating the role of nucleotide context in dictating ncAA incorporation efficiency (bacteria, mammalian cells and yeast) (Bartoschek et al., 2021; Pott et al., 2014; Potts et al., 2020; Stieglitz et al., 2021; Xu et al., 2016). Thus, identifying favorable sequence contexts that support enhanced ncAA incorporation efficiencies, as well as enhancing the performance of suppressor tRNAs, will be useful in improving overall efficiencies when adding two distinct ncAAs to the genetic code of yeast.

In addition to engineering individual translation components, genetic and genomic engineering approaches offer a complementary set of tools for further enhancing dual ncAA incorporation efficiency in yeast. In this work, we demonstrated that using single-gene deletion yeast strains *ppq1Δ* and *tpa1Δ* leads to significant improvements in ncAA incorporation in response to TGA across different OTSs, codon positions, and a range of ncAAs. The enhancements observed are consistent with the enhancements measured for ncAA incorporation in response to TAG in our previous work (Potts et al., 2020). Hence, utilizing such strains was both beneficial and straightforward for dual ncAA incorporation. Our findings also suggest that improving our fundamental understanding of eukaryotic protein biosynthesis may lead to further enhancements in genetic code manipulation in yeast (and other eukaryotes). Recently, our group reported a genome-wide screen to identify single-gene deletions that enhance ncAA incorporation efficiency in response to the amber (TAG) codon (Zackin et al., 2022). Out of the several dozen hits we identified, many of the genes have no known connections to protein biosynthesis, indicating that there are numerous routes available to engineer cells to enhance the efficiencies of dual ncAA incorporation strategies. Finally, bold genome engineering strategies such as the construction of a synthetic yeast genome (Sc2.0 project) free up codons for the addition of ncAAs to the genetic code (Annaluru et al., 2014; Sanders et al., 2022; Shen et al., 2022). “Blank” codons in such synthetic genomes are expected to greatly enhance the efficiency of ncAA incorporation and should be compatible with the dual ncAA incorporation machinery described in this work.

Conclusions

The yeast *S. cerevisiae* is one of the most important model organisms for elucidating fundamental biology and is a valuable chassis for protein engineering and synthetic biology. Thus, empowering yeast with the ability to encode multiple ncAAs in individual proteins will lead to exciting biotechnological advances including new classes of protein-based therapeutics, biomaterials, artificial enzymes, and biosensors. More fundamentally, elucidating the processes that support and enhance dual ncAA incorporation systems is expected to lead to a deeper understanding of eukaryotic translation processes and the identification of unknown factors that can enhance genetic code expansion in yeast. In our current work, the tools and conditions identified are indispensable elements for realizing such applications and provide general insights that can be applied to the implementation of multiple ncAA incorporation systems in additional eukaryotic cells and organisms.

Author Contributions

P.L. and J.A.V – Project conceptualization and experimental designs; P.L.- performed experiments and analyzed data; P.L.- wrote original manuscript draft; P.L. and J.A.V. – performed review and editing of the manuscript.

Conflicts of Interest

P.L. and J.A.V declare competing financial interests: A provisional patent application (Application No.- 63/319,729) has been filed by Tufts University for the dual ncAA incorporation systems described in this work. T2RS5, a variant of *Ec*TyrRS, and LysAlkRS3, a variant of *Ec*LeuRS used in this study, are sequence variants disclosed in a patent application filed by Tufts University- U.S. Patent Application No. PCT/US22/29775.

Acknowledgements

This research was supported by a grant from the National Institute of General Medical Sciences of the National Institutes of Health (1R35GM133471). The content of this work is solely the responsibility of the authors and does not necessarily represent the official views of the National Institutes of Health. The authors would also like to thank Heather Amoroso and Alla Leshinsky at the Koch Institute Biopolymers and Proteomics Core for their assistance with mass spectrometry data collection. Additionally, the authors would like to thank Rebecca Hershman and Briana Lino for their valuable feedback on the manuscript.

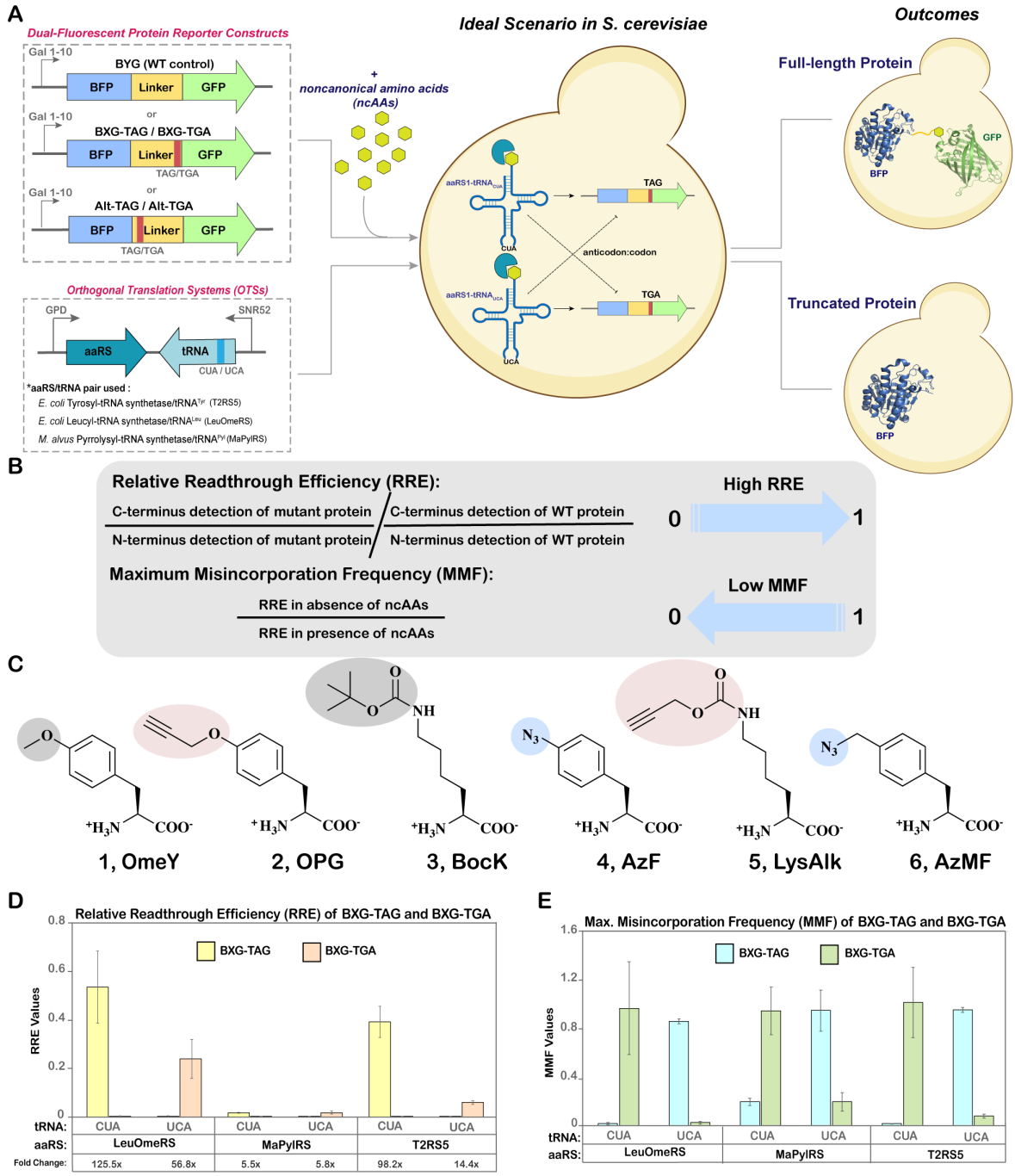

Figure 1. Evaluation of TAG versus TGA stop codon suppression. A) Schematic overview of dual plasmid approach outlining the architecture of dual-fluorescent reporter constructs and orthogonal translation system (OTS) constructs. The possible cognate and non-cognate codon:anticodon interactions of amber and opal suppressor tRNAs are shown as bold arrows and dotted lines, respectively. B) Equations used for determining relative readthrough efficiency (RRE) and maximum misincorporation frequency (MMF), quantitative parameters for evaluating ncAA incorporation efficiency and fidelity, respectively. C) Structures of ncAAs used in this study. Shaded regions highlight functional groups, some of which can undergo specific bioorthogonal reactions. **1**, *O*-methyl-L-tyrosine (OmeY); **2**, N^{ε}-Boc-L-Lysine (BocK); **3**, *p*-propargyloxyl-L-phenylalanine (OPG); **4**, *p*-azido-L-phenylalanine (AzF); **5**, N^{ε}-propargyloxycarbonyl-L-lysine (LysAlk); **6**, 4-azidomethyl-L-phenylalanine (AzMF). D) Relative Readthrough Efficiency (RRE) of BXG-TAG and BXG-TGA reporters with indicated tRNA and aaRS constructs calculated from flow cytometry experiments. The

fold changes reported below the plots (e.g. 125.5x) indicate the fold change in readthrough between BXG-TAG and BXG-TGA by a particular OTS; these values were calculated from the ratios of median fluorescence intensities (MFIs) of readthrough events of these reporter constructs (the larger value was used as the numerator). E) Maximum Misincorporation Frequency (MMF) calculated for BXG-TAG and BXG-TGA reporter constructs. Flow cytometry dot plots and and bar graphs of MFIs for all data in this figure are depicted in Figure S1 and Figure S2, respectively. The error bars in D and E were derived from measurements of biological triplicates, starting with standard deviations of MFI values and propagated using error propagation equations (during calculations of RRE and MMF).

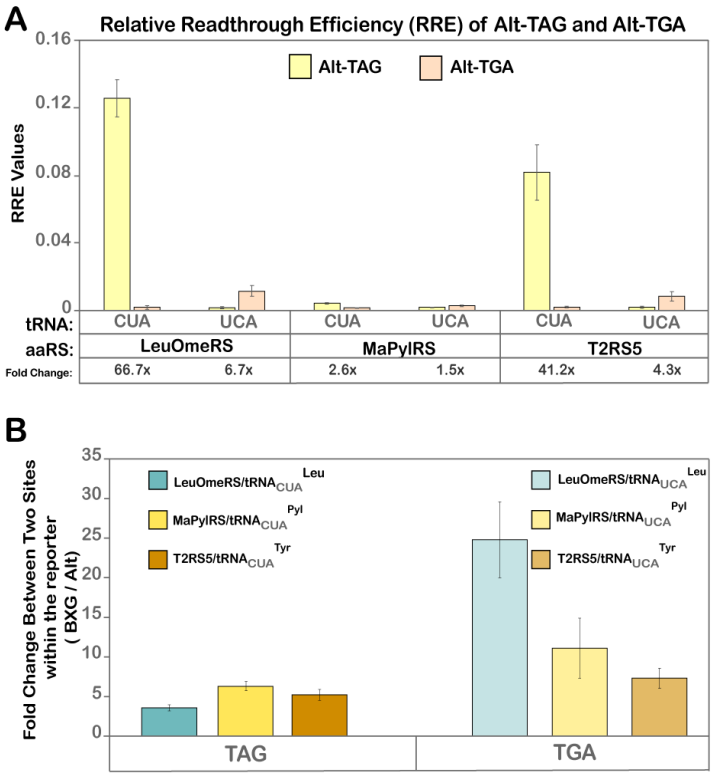

Figure 2. Quantitative analysis of readthrough events for Alt-TAG and Alt-TGA constructs. A) Relative Readthrough Efficiency (RRE) for Alt-TAG and Alt-TGA reporter constructs calculated from MFI values obtained from flow cytometry dot plot data, depicted in Figure S3. The fold-changes in readthrough (eg: 66.7X) in the table below indicate the fold change in readthrough between Alt-TAG and Alt-TGA by a particular OTS; these values were calculated from the ratios of MFIs of readthrough events of these reporter constructs (the larger value was used as the numerator). The corresponding MMF graph and the MFI bar graph are represented in Figure S4. B) Fold change in readthrough performance between the two codon positions in the reporter (BXG and Alt) obtained from the ratio of MFI values of cognate OTS:reporter interaction at the BXG-TAG (or BXG-TGA) site to the Alt-TAG (or Alt-TGA) site. The error bars in both A and B were calculated from the standard deviation of MFI values and then propagated in subsequent calculations using error propagation equations.

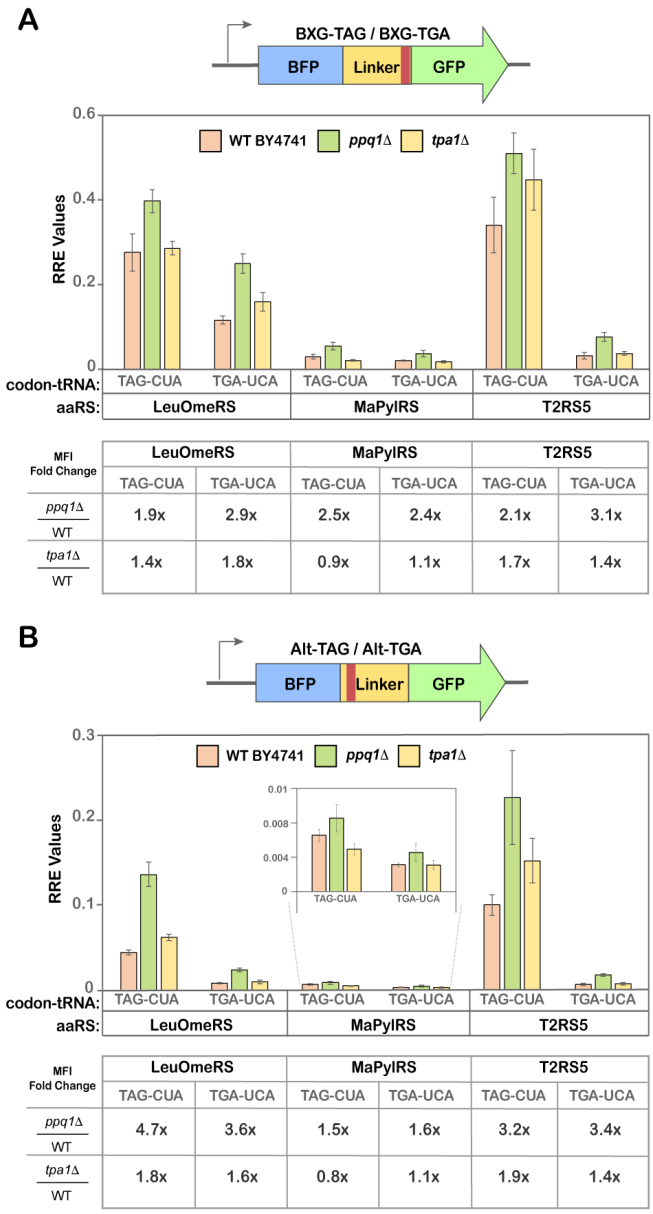

MFI Fold Change	LeuOmeRS		MaPylRS		T2RS5	
	TAG-CUA	TGA-UCA	TAG-CUA	TGA-UCA	TAG-CUA	TGA-UCA
ppq1Δ / WT	1.9x	2.9x	2.5x	2.4x	2.1x	3.1x
tpa1Δ / WT	1.4x	1.8x	0.9x	1.1x	1.7x	1.4x

MFI Fold Change	LeuOmeRS		MaPylRS		T2RS5	
	TAG-CUA	TGA-UCA	TAG-CUA	TGA-UCA	TAG-CUA	TGA-UCA
ppq1Δ / WT	4.7x	3.6x	1.5x	1.6x	3.2x	3.4x
tpa1Δ / WT	1.8x	1.6x	0.8x	1.1x	1.9x	1.4x

Figure 3. Quantitative readthrough measurements in single-gene knockout yeast strains. A) Relative Readthrough Efficiency (RRE) of BXG-TAG and BXG-TGA reporters with indicated tRNA and aaRS constructs calculated from flow cytometry experiments for the yeast strain BY4741 and single-gene knockouts *ppq1Δ* and *tpa1Δ*. B) Relative Readthrough Efficiency (RRE) of Alt-TAG and Alt-TGA reporters with indicated tRNA and aaRS constructs calculated from flow cytometry experiments for the yeast strain BY4741 and single-gene knockouts *ppq1Δ* and *tpa1Δ*. *O*-methyl-L-tyrosine (**1**; OmeY) was used as substrate for LeuOmeRS/tRNA^{Leu}, N^{ε}-Boc-L-Lysine (**2**; BocK) was used as a substrate for MaPylRS/tRNA^{Pyl}; and *p*-propargyloxyl-L-phenylalanine (**3**; OPG) was used as a substrate for T2RS5/tRNA^{Tyr}. The error bars are representative of three independent experiments, calculated from the standard deviations and processed through error propagation equations. The fold change in readthrough values (e.g. 1.9x) are represented in table format (below each RRE plot in A and B) and were obtained from the ratios of MFI values of a particular codon:OTS interaction in a knockout yeast strain to the corresponding MFI value in the WT BY4741 strain. The corresponding MMF graph and the MFI bar graphs for the data in this figure are depicted in supplementary Figure S8 and S9.

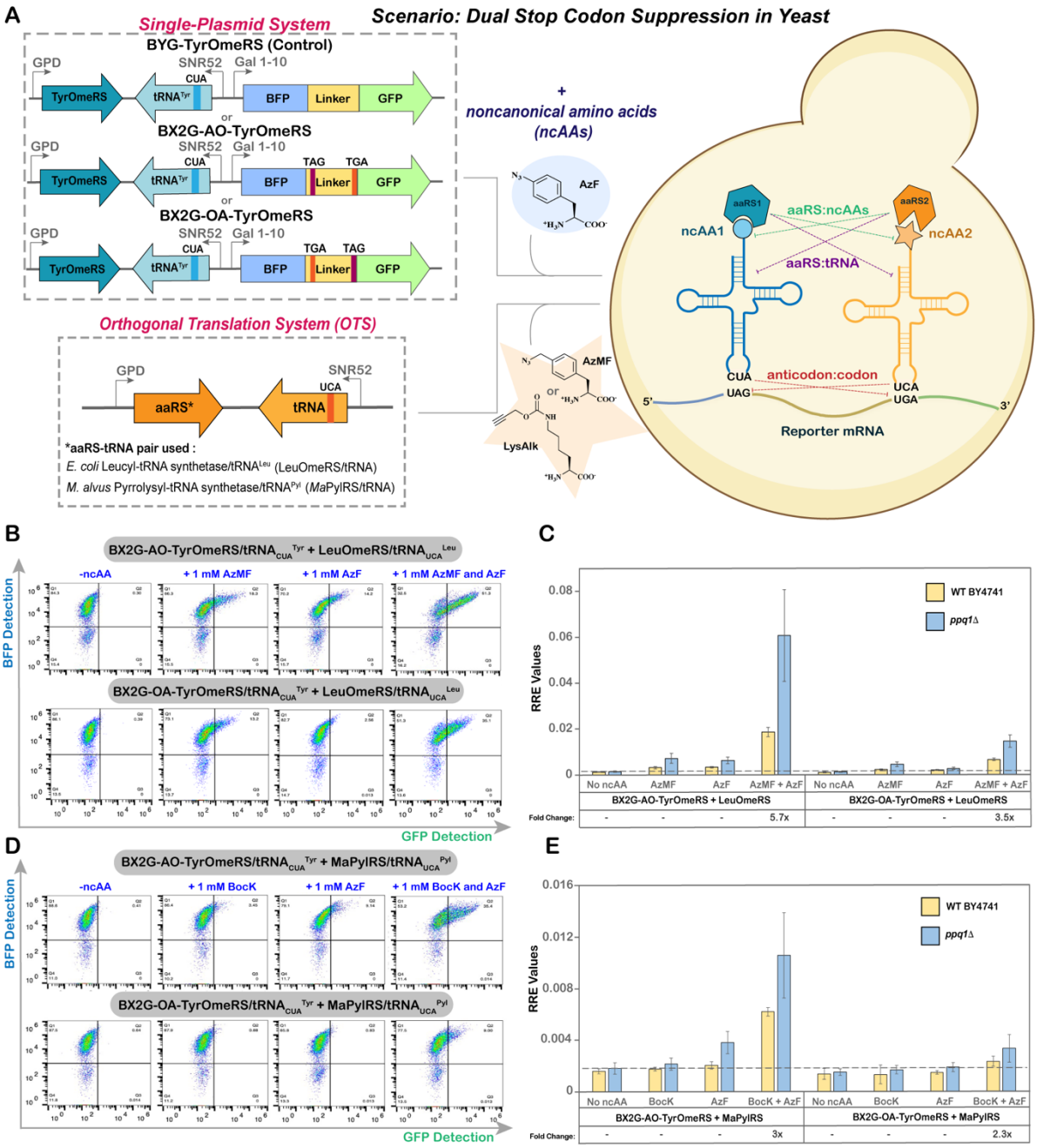

Figure 4. Evaluation of dual ncAA incorporation system in yeast. A) Experimental outline of dual plasmid approach to facilitate expression of two OTSs in the host cell. Dotted lines (---) and color-matched labels indicate potential non-cognate interactions that can occur. B) Flow cytometry dot plots of readthrough events of BX_2G-AO and BX_2G-OA in *ppq1Δ*, employing the OTS combination of *Ec*TyrRS/$tRNA_{CUA}^{Tyr}$ + *Ec*LeuRS/$tRNA_{UCA}^{Leu}$ and four different induction conditions. C) Corresponding Relative Readthrough Efficiency (RRE) calculated for OTS combination of *Ec*TyrRS/$tRNA_{CUA}^{Tyr}$ + *Ec*LeuRS/$tRNA_{UCA}^{Leu}$ for the reporters BX2G-AO and BX2G-OA in BY4741 and *ppq1Δ* strains. D) Flow cytometry dot plots of readthrough events of BX_2G-AO and BX_2G-OA in *ppq1Δ*, employing the OTS combination of *Ec*TyrRS/$tRNA_{CUA}^{Tyr}$ + *Ma*PylRS/$tRNA_{UCA}^{Pyl}$ and four different induction conditions. E) Corresponding Relative Readthrough Efficiency (RRE) measurements for the OTS combination of *Ec*TyrRS/$tRNA_{CUA}^{Tyr}$ + *Ma*PylRS/$tRNA_{UCA}^{Pyl}$ for the

reporters BX2G-AO and BX2G-OA in WT BY4741 and *ppq1Δ* strains. The error bars are representative of three independent experiments, calculated from the standard deviation values and processed through error propagation equations. The fold change in readthrough represented in the graphs (e.g. 6x; panels C and E) are obtained from the ratios of MFI values of readthrough events in *ppq1Δ* and BY4741 strains. Corresponding maximum misincorporation frequency (MMF) graphs can be found in Supplementary Figure S12.

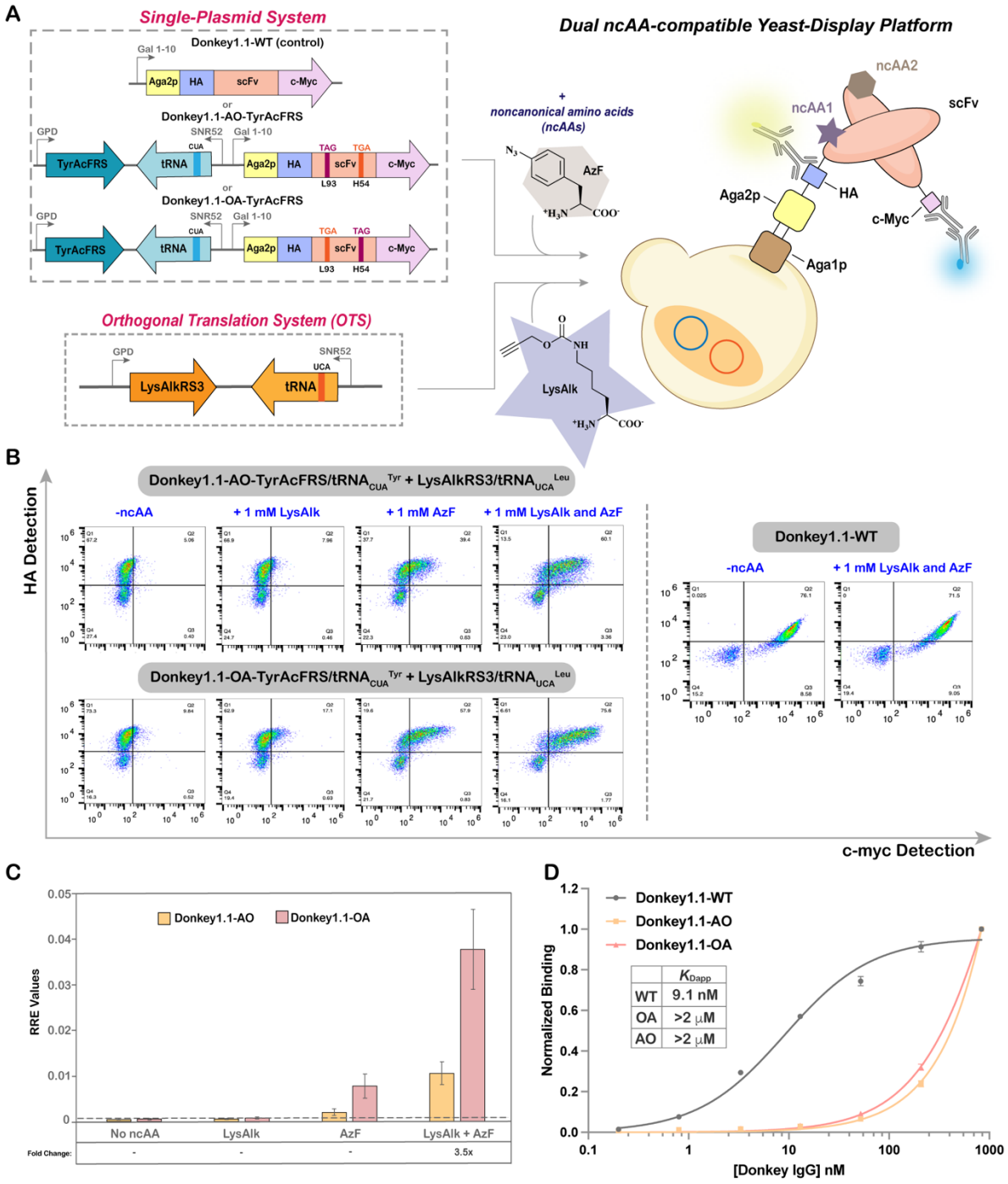

Figure 5. Evaluation of dual ncAA incorporation in yeast display format. A) Experimental outline for setting up a dual ncAA incorporation system with yeast-display platform. HA and c-Myc tags were employed to evaluate full-length readthrough of yeast-displayed scFvs using flow cytometry. B) Flow cytometry dot plots of readthrough experiments conducted in the RJY100 yeast display strain. Display

of Donkey1.1-AO, Donkey1.1-OA and Donkey1.1 WT reporters following induction in the presence of 0, 1, or 2 ncAAs. Donkey1.1-WT was used as a positive control. C) RRE measurements comparing readthrough efficiencies between Donkey1.1-AO and Donkey1.1-OA scFv reporters across different induction conditions. Errors bars are representative of experiments conducted with three biological replicates and were determined via error propagation. The fold changes in readthrough represented in the graph (e.g. 3.5x) were obtained from the ratio of MFI values of readthrough events of Donkey1.1-OA to Donkey1.1-AO by the OTS combination of *Ec*TyrRS/$tRNA_{CUA}^{Tyr}$ + *Ec*LeuRS/$tRNA_{UCA}^{Leu}$. The corresponding MMF data can be found in Supplementary Figure S13. D) Yeast display titration experiments with doubly substituted and WT synthetic antibody clones. The graph depicts normalized antigen binding levels of the three yeast-displayed scFvs obtained over a range of antigen concentrations using flow cytometry. Corresponding dot plots can be found in Supplementary Figure S14.

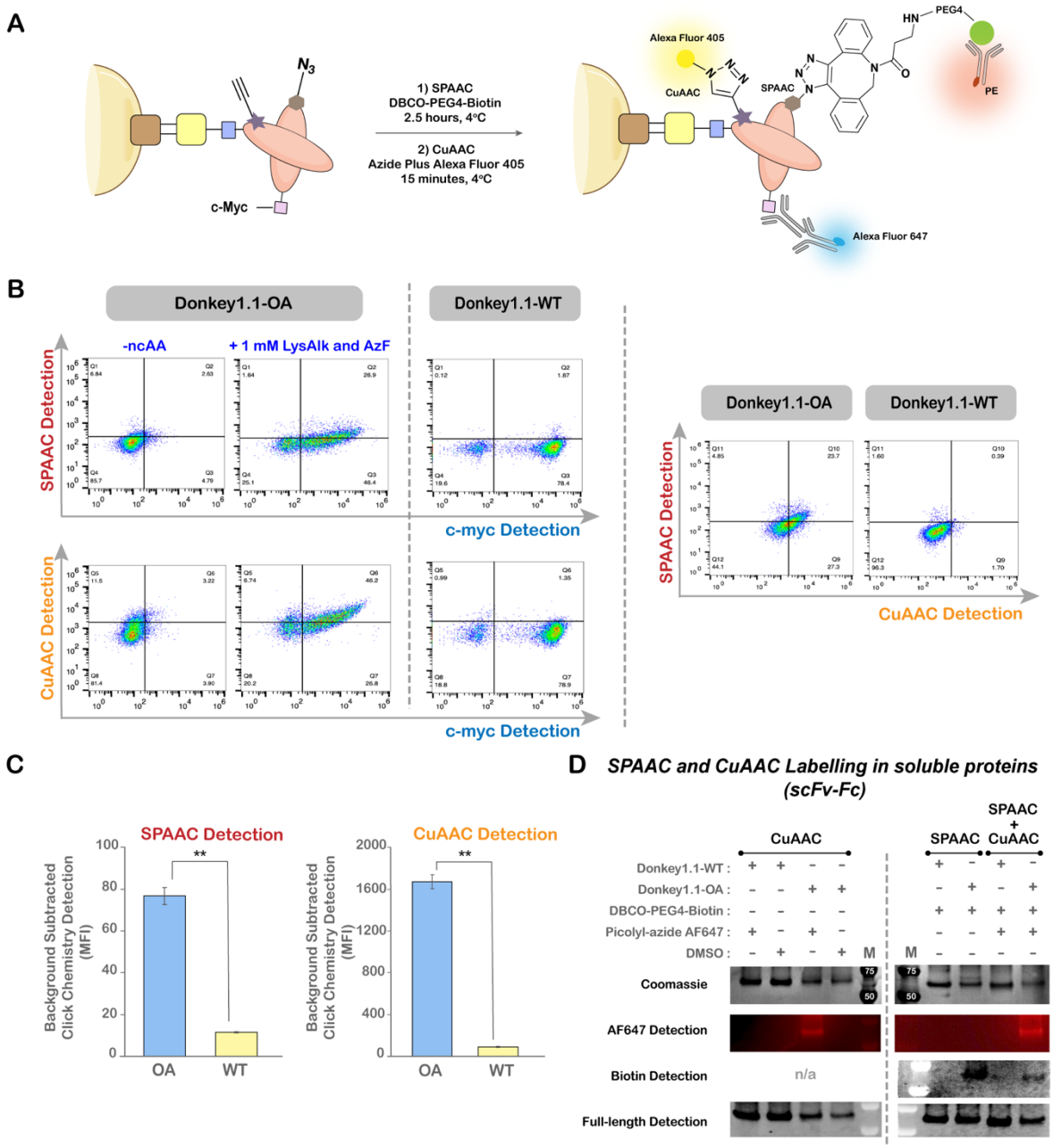

Figure 6: Site-specific double labeling of yeast-displayed and soluble proteins. A) Reaction and detection schemes for double labeling of yeast displayed, doubly substituted antibody constructs. TAG was employed to encode AzF (**4**; SPAAC reactions), while TGA was employed to encode LysAlk (**5**; CuAAC reactions). SPAAC products were detected using a PE-labeled anti-biotin antibody, CuAAC reaction products were detected with an Alexa Fluor 405-labeled azide probe, and c-myc (full length proteins) was detected using an anti-c-myc primary antibody followed by an Alexa Fluor 647-labeled secondary antibody. B) Flow cytometry dot plots of SPAAC and CuAAC reactions along with full-length (c-myc) display detection for Donkey1.1-OA under different induction conditions. Donkey1.1-WT (no ncAA substitutions) served as a negative control. C) Median fluorescence intensities of SPAAC and CuAAC reaction products in c-myc+ populations for Donkey1.1-OA and Donkey1.1-WT constructs. Error bars denote standard deviations obtained from three independent experiments. Unpaired t-tests were performed to evaluate statistical significance (**: $p<0.005$). D) Single and double labeling of soluble Donkey1.1-OA and Donkey1.1-WT scFv-Fcs. SPAAC was performed using a DBCO-PEG4-biotin probe and detected by western blot using Streptavidin 488. CuAAC was performed

using Picolyl-azide Alexa Fluor 647 and detected by fluorescent gel imaging. Full-length protein expression was detected by western blot using goat anti-human IgG Fc Dy488. Coomassie staining was performed to verify sample purity. “M” indicates gel lane with molecular weight marker.

References:

Alcala-Torano, R., Islam, M., Cika, J., Lam, K.H., Jin, R., Ichtchenko, K., Shoemaker, C., and Van Deventer, J. (2022). Yeast Display Enables Identification of Covalent Single Domain Antibodies Against Botulinum Neurotoxin Light Chain A. chemRxiv. https://doi.org/10.26434/chemrxiv-2022-lrj2r.

Amiram, M., Haimovich, A.D., Fan, C., Wang, Y.-S., Aerni, H.-R., Ntai, I., Moonan, D.W., Ma, N.J., Rovner, A.J., Hong, S.H., et al. (2015). Evolution of translation machinery in recoded bacteria enables multi-site incorporation of nonstandard amino acids. Nat Biotechnol *33*, 1272–1279. https://doi.org/10.1038/nbt.3372.

Annaluru, N., Muller, H., Mitchell, L.A., Ramalingam, S., Stracquadanio, G., Richardson, S.M., Dymond, J.S., Kuang, Z., Scheifele, L.Z., Cooper, E.M., et al. (2014). Total Synthesis of a Functional Designer Eukaryotic Chromosome. Science *344*, 55–58. https://doi.org/10.1126/science.1249252.

Anzalone, A.V., Zairis, S., Lin, A.J., Rabadan, R., and Cornish, V.W. (2019). Interrogation of Eukaryotic Stop Codon Readthrough Signals by in Vitro RNA Selection. Biochemistry *58*, 1167–1178. https://doi.org/10.1021/acs.biochem.8b01280.

Bartoschek, M.D., Ugur, E., Nguyen, T.-A., Rodschinka, G., Wierer, M., Lang, K., and Bultmann, S. (2021). Identification of permissive amber suppression sites for efficient non-canonical amino acid incorporation in mammalian cells. Nucleic Acids Res *49*, e62. https://doi.org/10.1093/nar/gkab132.

Bednar, R.M., Jana, S., Kuppa, S., Franklin, R., Beckman, J., Antony, E., Cooley, R.B., and Mehl, R.A. (2021). Genetic Incorporation of Two Mutually Orthogonal Bioorthogonal Amino Acids That Enable Efficient Protein Dual-Labeling in Cells. ACS Chem. Biol. *16*, 2612–2622. https://doi.org/10.1021/acschembio.1c00649.

Beránek, V., Reinkemeier, C.D., Zhang, M.S., Liang, A.D., Kym, G., and Chin, J.W. (2018). Genetically Encoded Protein Phosphorylation in Mammalian Cells. Cell Chemical Biology *25*, 1067-1074.e5. https://doi.org/10.1016/j.chembiol.2018.05.013.

Beránek, V., Willis, J.C.W., and Chin, J.W. (2019). An Evolved Methanomethylophilus alvus Pyrrolysyl-tRNA Synthetase/tRNA Pair Is Highly Active and Orthogonal in Mammalian Cells. Biochemistry *58*, 387–390. https://doi.org/10.1021/acs.biochem.8b00808.

Beznosková, P., Gunišová, S., and Valášek, L.S. (2016). Rules of UGA-N decoding by near-cognate tRNAs and analysis of readthrough on short uORFs in yeast. RNA *22*, 456–466. https://doi.org/10.1261/rna.054452.115.

Beznosková, P., Pavlíková, Z., Zeman, J., Echeverría Aitken, C., and Valášek, L.S. (2019). Yeast applied readthrough inducing system (YARIS): an invivo assay for the comprehensive study of translational readthrough. Nucleic Acids Research *47*, 6339–6350. https://doi.org/10.1093/nar/gkz346.

Biddle, W., Schwark, D.G., Schmitt, M.A., and Fisk, J.D. (2022). Directed Evolution Pipeline for the Improvement of Orthogonal Translation Machinery for Genetic Code Expansion at Sense Codons. Frontiers in Chemistry *10*:815788. https://doi.org/10.3389/fchem.2022.815788.

Blanchet, S., Cornu, D., Argentini, M., and Namy, O. (2014). New insights into the incorporation of natural suppressor tRNAs at stop codons in Saccharomyces cerevisiae. Nucleic Acids Res *42*, 10061–10072. https://doi.org/10.1093/nar/gku663.

Botstein, D., and Fink, G.R. (2011). Yeast: An Experimental Organism for 21st Century Biology. Genetics *189*, 695–704. https://doi.org/10.1534/genetics.111.130765.

Cervettini, D., Tang, S., Fried, S.D., Willis, J.C.W., Funke, L.F.H., Colwell, L.J., and Chin, J.W. (2020). Rapid discovery and evolution of orthogonal aminoacyl-tRNA synthetase–tRNA pairs. Nat Biotechnol *38*, 989–999. https://doi.org/10.1038/s41587-020-0479-2.

Chao, G., Lau, W.L., Hackel, B.J., Sazinsky, S.L., Lippow, S.M., and Wittrup, K.D. (2006). Isolating and engineering human antibodies using yeast surface display. Nat Protoc *1*, 755–768. https://doi.org/10.1038/nprot.2006.94.

Chen, Y., He, X., Ma, B., Liu, K., Gao, T., Niu, W., and Guo, J. (2022). Noncanonical amino acid mutagenesis in response to recoding signal-enhanced quadruplet codons. Nucleic Acids Research gkac474. https://doi.org/10.1093/nar/gkac474.

Cherf, G.M., and Cochran, J.R. (2015). Applications of yeast surface display for protein engineering. Methods Mol Biol *1319*, 155–175. https://doi.org/10.1007/978-1-4939-2748-7_8.

Chin, J.W., Cropp, T. A., Anderson, J. C., Mukherji, M., Zhang, Z. W., and Schultz, P. G. (2003). An Expanded Eukaryotic Genetic Code. Science *301*, 964–967. https://doi.org/10.1126/science.1084772.

Chin, J.W. (2014). Expanding and Reprogramming the Genetic Code of Cells and Animals. Annu. Rev. Biochem. *83*, 379–408. https://doi.org/10.1146/annurev-biochem-060713-035737.

Chung, C.Z., Amikura, K., and Söll, D. (2020). Using Genetic Code Expansion for Protein Biochemical Studies. Front Bioeng Biotechnol *8*. https://doi.org/10.3389/fbioe.2020.598577.

Cui, Z., Mureev, S., Polinkovsky, M.E., Tnimov, Z., Guo, Z., Durek, T., Jones, A., and Alexandrov, K. (2017). Combining Sense and Nonsense Codon Reassignment for Site-Selective Protein Modification with Unnatural Amino Acids. ACS Synth. Biol. *6*, 535–544. https://doi.org/10.1021/acssynbio.6b00245.

Dabrowski, M., Bukowy-Bieryllo, Z., and Zietkiewicz, E. (2015). Translational readthrough potential of natural termination codons in eucaryotes – The impact of RNA sequence. RNA Biol *12*, 950–958. https://doi.org/10.1080/15476286.2015.1068497.

DeBenedictis, E.A., Carver, G.D., Chung, C.Z., Söll, D., and Badran, A.H. (2021). Multiplex suppression of four quadruplet codons via tRNA directed evolution. Nat Commun *12*, 5706. https://doi.org/10.1038/s41467-021-25948-y.

Ding, W., Zhao, H., Chen, Y., Zhang, B., Yang, Y., Zang, J., Wu, J., and Lin, S. (2020). Chimeric design of pyrrolysyl-tRNA synthetase/tRNA pairs and canonical synthetase/tRNA pairs for genetic code expansion. Nat Commun *11*, 3154. https://doi.org/10.1038/s41467-020-16898-y.

Dumas, A., Lercher, L., Spicer, C.D., and Davis, B.G. (2015). Designing logical codon reassignment – Expanding the chemistry in biology. Chem. Sci. *6*, 50–69. https://doi.org/10.1039/C4SC01534G.

Dunkelmann, D.L., Willis, J.C.W., Beattie, A.T., and Chin, J.W. (2020). Engineered triply orthogonal pyrrolysyl–tRNA synthetase/tRNA pairs enable the genetic encoding of three distinct non-canonical amino acids. Nat. Chem. *12*, 535–544. https://doi.org/10.1038/s41557-020-0472-x.

Dunkelmann, D.L., Oehm, S.B., Beattie, A.T., and Chin, J.W. (2021). A 68-codon genetic code to incorporate four distinct non-canonical amino acids enabled by automated orthogonal mRNA design. Nat. Chem. 1–8. https://doi.org/10.1038/s41557-021-00764-5.

Fan, C., Xiong, H., Reynolds, N.M., and Söll, D. (2015). Rationally evolving tRNAPyl for efficient incorporation of noncanonical amino acids. Nucleic Acids Res *43*, e156. https://doi.org/10.1093/nar/gkv800.

Fischer, J.T., Söll, D., and Tharp, J.M. (2022). Directed Evolution of Methanomethylophilus alvus Pyrrolysyl-tRNA Synthetase Generates a Hyperactive and Highly Selective Variant. Frontiers in Molecular Biosciences *9*:850613. https://doi.org/10.3389/fmolb.2022.850613.

Gan, R., Perez, J.G., Carlson, E.D., Ntai, I., Isaacs, F.J., Kelleher, N.L., and Jewett, M.C. (2017). Translation system engineering in *Escherichia coli* enhances non-canonical amino acid incorporation into proteins. Biotechnol. Bioeng. *114*, 1074–1086. https://doi.org/10.1002/bit.26239.

Giaever, G., and Nislow, C. (2014). The Yeast Deletion Collection: A Decade of Functional Genomics. Genetics *197*, 451–465. https://doi.org/10.1534/genetics.114.161620.

Grasso, K.T., Singha Roy, S.J., Osgood, A.O., Yeo, M.J.R., Soni, C., Hillenbrand, C.M., Ficaretta, E.D., and Chatterjee, A. (2022). A Facile Platform to Engineer Escherichia coli Tyrosyl-tRNA Synthetase Adds New Chemistries to the Eukaryotic Genetic Code, Including a Phosphotyrosine Mimic. ACS Cent. Sci. https://doi.org/10.1021/acscentsci.1c01465.

Guo, J., Melançon III, C.E., Lee, H.S., Groff, D., and Schultz, P.G. (2009). Evolution of Amber Suppressor tRNAs for Efficient Bacterial Production of Proteins Containing Nonnatural Amino Acids. Angewandte Chemie International Edition *48*, 9148–9151. https://doi.org/10.1002/anie.200904035.

von der Haar, T., and Tuite, M.F. (2007). Regulated translational bypass of stop codons in yeast. Trends in Microbiology *15*, 78–86. https://doi.org/10.1016/j.tim.2006.12.002.

Hancock, S.M., Uprety, R., Deiters, A., and Chin, J.W. (2010). Expanding the Genetic Code of Yeast for Incorporation of Diverse Unnatural Amino Acids via a Pyrrolysyl-tRNA Synthetase/tRNA Pair. J. Am. Chem. Soc. *132*, 14819–14824. https://doi.org/10.1021/ja104609m.

Hankore, E.D., Zhang, L., Chen, Y., Liu, K., Niu, W., and Guo, J. (2019). Genetic Incorporation of Noncanonical Amino Acids Using Two Mutually Orthogonal Quadruplet Codons. ACS Synth. Biol. *8*, 1168–1174. https://doi.org/10.1021/acssynbio.9b00051.

He, X., Chen, Y., Beltran, D.G., Kelly, M., Ma, B., Lawrie, J., Wang, F., Dodds, E., Zhang, L., Guo, J., et al. (2020). Functional genetic encoding of sulfotyrosine in mammalian cells. Nat Commun *11*, 4820. https://doi.org/10.1038/s41467-020-18629-9.

Hershman, R.L., Li, Y., Ma, F., Xu, Q., and Van Deventer, J.A. (2022). Intracellular Delivery of Antibodies for Selective Cell Signaling Interference. ChemMedChem *17*, e202100678. https://doi.org/10.1002/cmdc.202100678.

Hohl, A., Karan, R., Akal, A., Renn, D., Liu, X., Ghorpade, S., Groll, M., Rueping, M., and Eppinger, J. (2019). Engineering a Polyspecific Pyrrolysyl-tRNA Synthetase by a High Throughput FACS Screen. Sci Rep *9*, 11971. https://doi.org/10.1038/s41598-019-48357-0.

Holstein, J.M., Muttach, F., Schiefelbein, S.H.H., and Rentmeister, A. (2017). Dual 5′ Cap Labeling Based on Regioselective RNA Methyltransferases and Bioorthogonal Reactions. Chemistry – A European Journal *23*, 6165–6173. https://doi.org/10.1002/chem.201604816.

Islam, M., Kehoe, H.P., Lissoos, J.B., Huang, M., Ghadban, C.E., Berumen Sánchez, G., Lane, H.Z., and Van Deventer, J.A. (2021). Chemical Diversification of Simple Synthetic Antibodies. ACS Chem. Biol. *16*, 344–359. https://doi.org/10.1021/acschembio.0c00865.

Italia, J.S., Addy, P.S., Wrobel, C.J.J., Crawford, L.A., Lajoie, M.J., Zheng, Y., and Chatterjee, A. (2017). An orthogonalized platform for genetic code expansion in both bacteria and eukaryotes. Nat Chem Biol *13*, 446–450. https://doi.org/10.1038/nchembio.2312.

Italia, J.S., Addy, P.S., Erickson, S.B., Peeler, J.C., Weerapana, E., and Chatterjee, A. (2019). Mutually Orthogonal Nonsense-Suppression Systems and Conjugation Chemistries for Precise Protein Labeling at up to Three Distinct Sites. J. Am. Chem. Soc. *141*, 6204–6212. https://doi.org/10.1021/jacs.8b12954.

Italia, J.S., Latour, C., Wrobel, C.J.J., and Chatterjee, A. (2018). Resurrecting the Bacterial Tyrosyl-tRNA Synthetase/tRNA Pair for Expanding the Genetic Code of Both E. coli and Eukaryotes. Cell Chem. Biol. *25*, 1304-1312. https://doi.org/10.1016/j.chembiol.2018.07.002

Jones, C.M., Robkis, D.M., Blizzard, R.J., Munari, M., Venkatesh, Y., Mihaila, T.S., Eddins, A.J., Mehl, R.A., Zagotta, W.N., Gordon, S.E., et al. (2021). Genetic encoding of a highly photostable, long lifetime fluorescent amino acid for imaging in mammalian cells. Chem. Sci. https://doi.org/10.1039/D1SC01914G.

Keeling, K.M., Salas-Marco, J., Osherovich, L.Z., and Bedwell, D.M. (2006). Tpa1p is part of an mRNP complex that influences translation termination, mRNA deadenylation, and mRNA turnover in Saccharomyces cerevisiae. Mol Cell Biol *26*, 5237–5248. https://doi.org/10.1128/MCB.02448-05.

Kelemen, R., Jewel, D., Huang, R., Zhu, Z., Cao, X., Pasha, M., Anthony, J., Opijnen, T. van, and Chatterjee, A. (2022). Virus-assisted directed evolution of enhanced suppressor tRNAs in mammalian cells. bioRxiv. https://doi.org/10.1101/2022.01.21.477302

Kleiner, R.E., Ti, S.C., and Kapoor, T.M. (2013). Site-Specific Chemistry on the Microtubule Polymer. J. Am. Chem. Soc. *135*, 12520–12523. https://doi.org/10.1021/ja405199h.

Kohli, J., Kwong, T., Altruda, F., Söll, D., and Wahl, G. (1979). Characterization of a UGA-suppressing serine tRNA from Schizosaccharomyces pombe with the help of a new in vitro

assay system for eukaryotic suppressor tRNAs. Journal of Biological Chemistry *254*, 1546–1551. https://doi.org/10.1016/S0021-9258(17)37806-7.

Kunjapur, A.M., Stork, D.A., Kuru, E., Vargas-Rodriguez, O., Landon, M., Soll, D., and Church, G.M. (2018). Engineering posttranslational proofreading to discriminate nonstandard amino acids. Proceedings of the National Academy of Sciences *115*, 619-624. https://doi.org/10.1073/pnas.1715137115.

Lang, K., Davis, L., Wallace, S., Mahesh, M., Cox, D.J., Blackman, M.L., Fox, J.M., and Chin, J.W. (2012). Genetic Encoding of Bicyclononynes and trans-Cyclooctenes for Site-Specific Protein Labeling in Vitro and in Live Mammalian Cells via Rapid Fluorogenic Diels–Alder Reactions. J. Am. Chem. Soc. *134*, 10317–10320. https://doi.org/10.1021/ja302832g.

Lewis, A.K., Harthorn, A., Johnson, S.M., Lobb, R.R., and Hackel, B.J. (2021). Engineered protein-small molecule conjugates empower selective enzyme inhibition. Cell Chemical Biology https://doi.org/10.1016/j.chembiol.2021.07.013.

Li, X., and Liu, C.C. (2014). Biological Applications of Expanded Genetic Codes. ChemBioChem *15*, 2335–2341. https://doi.org/10.1002/cbic.201402159.

Li, Y., Hoskins, J.N., Sreerama, S.G., and Grayson, S.M. (2010). MALDI-TOF Mass Spectral Characterization of Polymers Containing an Azide Group: Evidence of Metastable Ions. Macromolecules *43*, 6225–6228. https://doi.org/10.1021/ma100599n.

Lion, C., Simon, C., Huss, B., Blervacq, A.-S., Tirot, L., Toybou, D., Spriet, C., Slomianny, C., Guerardel, Y., Hawkins, S., et al. (2017). BLISS: A Bioorthogonal Dual-Labeling Strategy to Unravel Lignification Dynamics in Plants. Cell Chemical Biology *24*, 326–338. https://doi.org/10.1016/j.chembiol.2017.02.009.

Macino, G., Coruzzi, G., Nobrega, F.G., Li, M., and Tzagoloff, A. (1979). Use of the UGA terminator as a tryptophan codon in yeast mitochondria. Proceedings of the National Academy of Sciences *76*, 3784–3785. https://doi.org/10.1073/pnas.76.8.3784.

Mattanovich, D., Branduardi, P., Dato, L., Gasser, B., Sauer, M., and Porro, D. (2012). Recombinant protein production in yeasts. Methods Mol Biol *824*, 329–358. https://doi.org/10.1007/978-1-61779-433-9_17.

Maurel, D., Comps-Agrar, L., Brock, C., Rives, M.-L., Bourrier, E., Ayoub, M.A., Bazin, H., Tinel, N., Durroux, T., Prézeau, L., et al. (2008). Cell-surface protein-protein interaction analysis with time-resolved FRET and snap-tag technologies: application to GPCR oligomerization. Nat Methods *5*, 561–567. https://doi.org/10.1038/nmeth.1213.

McCaughan, K.K., Brown, C.M., Dalphin, M.E., Berry, M.J., and Tate, W.P. (1995). Translational termination efficiency in mammals is influenced by the base following the stop codon. Proc. Natl. Acad. Sci. U.S.A. *92*, 5431–5435. https://doi.org/10.1073/pnas.92.12.5431.

McMahon, C., Baier, A.S., Pascolutti, R., Wegrecki, M., Zheng, S., Ong, J.X., Erlandson, S.C., Hilger, D., Rasmussen, S.G.F., Ring, A.M., et al. (2018). Yeast surface display platform for rapid discovery of conformationally selective nanobodies. Nat Struct Mol Biol *25*, 289–296. https://doi.org/10.1038/s41594-018-0028-6.

Meineke, B., Heimgärtner, J., Lafranchi, L., and Elsässer, S.J. (2018). Methanomethylophilus alvus Mx1201 Provides Basis for Mutual Orthogonal Pyrrolysyl tRNA/Aminoacyl-tRNA Synthetase Pairs in Mammalian Cells. ACS Chem. Biol. *13*, 3087–3096. https://doi.org/10.1021/acschembio.8b00571.

Meineke, B., Heimgärtner, J., Eirich, J., Landreh, M., and Elsässer, S.J. (2020). Site-Specific Incorporation of Two ncAAs for Two-Color Bioorthogonal Labeling and Crosslinking of Proteins on Live Mammalian Cells. Cell Reports *31*, 107811. https://doi.org/10.1016/j.celrep.2020.107811.

Mukai, T., Kobayashi, T., Hino, N., Yanagisawa, T., Sakamoto, K., and Yokoyama, S. (2008). Adding l-lysine derivatives to the genetic code of mammalian cells with engineered pyrrolysyl-tRNA synthetases. Biochemical and Biophysical Research Communications *371*, 818–822. https://doi.org/10.1016/j.bbrc.2008.04.164.

Niu, W., Schultz, P.G., and Guo, J. (2013). An Expanded Genetic Code in Mammalian Cells with a Functional Quadruplet Codon. ACS Chem. Biol. *8*, 1640–1645. https://doi.org/10.1021/cb4001662.

Oller-Salvia, B., and Chin, J.W. (2019). Efficient Phage Display with Multiple Distinct Non-Canonical Amino Acids Using Orthogonal Ribosome-Mediated Genetic Code Expansion. Angew Chem Int Ed Engl *58*, 10844–10848. https://doi.org/10.1002/anie.201902658.

Osgood, A.O., Zheng, Y., Roy, S.J.S., Loynd, C., Jewel, D., and Chatterjee, A. (2022). An efficient opal-suppressor tryptophanyl pair creates new routes for simultaneously incorporating up to three distinct noncanonical amino acids into proteins in mammalian cells. bioRxiv. https://doi.org/10.1101/2022.08.02.502539

Petranovic, D., Tyo, K., Vemuri, G.N., and Nielsen, J. (2010). Prospects of yeast systems biology for human health: integrating lipid, protein and energy metabolism. FEMS Yeast Research *10*, 1046–1059. https://doi.org/10.1111/j.1567-1364.2010.00689.x.

Pott, M., Schmidt, M.J., and Summerer, D. (2014). Evolved Sequence Contexts for Highly Efficient Amber Suppression with Noncanonical Amino Acids. ACS Chem. Biol. *9*, 2815–2822. https://doi.org/10.1021/cb5006273.

Potts, K.A., Stieglitz, J.T., Lei, M., and Van Deventer, J.A.V. (2020). Reporter system architecture affects measurements of noncanonical amino acid incorporation efficiency and fidelity. Mol. Syst. Des. Eng. *5*, 573–588. https://doi.org/10.1039/C9ME00107G.

Ren, C., Wu, Q., Xiao, R., Ji, Y., Yang, X., Zhang, Z., Qin, H., Ma, J.-A., and Xuan, W. Expanding the Scope of Genetically Encoded Lysine PTMs with Lactylation, β-Hydroxybutyrylation and Lipoylation. ChemBioChem *n/a*. https://doi.org/10.1002/cbic.202200302.

Reynolds, N.M., Vargas-Rodriguez, O., Söll, D., and Crnković, A. (2017). The central role of tRNA in genetic code expansion. Biochim Biophys Acta *1861*, 3001–3008. https://doi.org/10.1016/j.bbagen.2017.03.012.

Row, R.D., and Prescher, J.A. (2018). Constructing New Bioorthogonal Reagents and Reactions. Acc. Chem. Res. *51*, 1073–1081. https://doi.org/10.1021/acs.accounts.7b00606.

Sachdeva, A., Wang, K., Elliott, T., and Chin, J.W. (2014). Concerted, Rapid, Quantitative, and Site-Specific Dual Labeling of Proteins. J. Am. Chem. Soc. *136*, 7785–7788. https://doi.org/10.1021/ja4129789.

Sanders, J., Hoffmann, S.A., Green, A.P., and Cai, Y. (2022). New opportunities for genetic code expansion in synthetic yeast. Current Opinion in Biotechnology *75*, 102691. https://doi.org/10.1016/j.copbio.2022.102691.

Schmied, W.H., Elsässer, S.J., Uttamapinant, C., and Chin, J.W. (2014). Efficient Multisite Unnatural Amino Acid Incorporation in Mammalian Cells via Optimized Pyrrolysyl tRNA Synthetase/tRNA Expression and Engineered eRF1. J. Am. Chem. Soc. *136*, 15577–15583. https://doi.org/10.1021/ja5069728.

Shandell, M.A., Tan, Z., and Cornish, V.W. (2021). Genetic Code Expansion: A Brief History and Perspective. Biochemistry *60*, 3455–3469. https://doi.org/10.1021/acs.biochem.1c00286.

Sharma, V., Zeng, Y., Wang, W.W., Qiao, Y., Kurra, Y., and Liu, W.R. (2018). Evolving the N-Terminal Domain of Pyrrolysyl-tRNA Synthetase for Improved Incorporation of Noncanonical Amino Acids. ChemBioChem *19*, 26–30. https://doi.org/10.1002/cbic.201700268.

Shen, Y. et al. (2022). Dissecting aneuploidy phenotypes by constructing Sc2.0 chromosome VII and SCRaMbLEing synthetic disomic yeast. bioRxiv. https://doi.org/10.1101/2022.09.01.506252

Simon, C., Lion, C., Spriet, C., Baldacci-Cresp, F., Hawkins, S., and Biot, C. (2018). One, Two, Three: A Bioorthogonal Triple Labelling Strategy for Studying the Dynamics of Plant Cell Wall Formation In Vivo. Angewandte Chemie *130*, 16907–16913. https://doi.org/10.1002/ange.201808493.

Smith, M.G., and Snyder, M. (2006). Yeast as a model for human disease. Curr Protoc Hum Genet *Chapter 15*, Unit 15.6. https://doi.org/10.1002/0471142905.hg1506s48.

Song, J.M., and Liebman, S.W. (1987). Allosuppressors that enhance the efficiency of omnipotent suppressors in *Saccharomyces cerevisiae*. Genetics *115*, 451–460. https://doi.org/10.1093/genetics/115.3.451.

Stieglitz, J.T., and Van Deventer, J.A. (2022). High-Throughput Aminoacyl-tRNA Synthetase Engineering for Genetic Code Expansion in Yeast. ACS Synth. Biol. https://doi.org/10.1021/acssynbio.1c00626.

Stieglitz, J.T., Kehoe, H.P., Lei, M., and Van Deventer, J.A. (2018). A Robust and Quantitative Reporter System To Evaluate Noncanonical Amino Acid Incorporation in Yeast. ACS Synth. Biol. *7*, 2256–2269. https://doi.org/10.1021/acssynbio.8b00260.

Stieglitz, J.T., Potts, K.A., and Deventer, J.A.V. (2021). Broadening the toolkit for quantitatively evaluating noncanonical amino acid incorporation in yeast. BioRxiv 2021.08.02.454837. https://doi.org/10.1101/2021.08.02.454837.

Stieglitz, J.T., Lahiri, P., Stout, M.I., and Van Deventer, J.A. (2022). Exploration of Methanomethylophilus alvus Pyrrolysyl-tRNA Synthetase Activity in Yeast. ACS Synth. Biol. *11*, 1824–1834. https://doi.org/10.1021/acssynbio.2c00001.

Tan, L., Zheng, Z., Xu, Y., Kong, W., Dai, Z., Qin, X., Liu, T., and Tang, H. (2020). Efficient Selection Scheme for Incorporating Noncanonical Amino Acids Into Proteins in Saccharomyces cerevisiae. Front. Bioeng. Biotechnol. *8*, 569191. https://doi.org/10.3389/fbioe.2020.569191.

Tharp, J.M., Vargas-Rodriguez, O., Schepartz, A., and Söll, D. (2021). Genetic Encoding of Three Distinct Noncanonical Amino Acids Using Reprogrammed Initiator and Nonsense Codons. ACS Chem. Biol. https://doi.org/10.1021/acschembio.1c00120.

de la Torre, D., and Chin, J.W. (2021). Reprogramming the genetic code. Nat Rev Genet *22*, 169–184. https://doi.org/10.1038/s41576-020-00307-7.

Trotta, E. (2013). Selection on codon bias in yeast: a transcriptional hypothesis. Nucleic Acids Res *41*, 9382–9395. https://doi.org/10.1093/nar/gkt740.

Truong, F., Yoo, T.H., Lampo, T.J., and Tirrell, D.A. (2012). Two-strain, cell-selective protein labeling in mixed bacterial cultures. J Am Chem Soc *134*, 8551–8556. https://doi.org/10.1021/ja3004667.

Uhlenbeck, O.C., and Schrader, J.M. (2018). Evolutionary tuning impacts the design of bacterial tRNAs for the incorporation of unnatural amino acids by ribosomes. Current Opinion in Chemical Biology *46*, 138–145. https://doi.org/10.1016/j.cbpa.2018.07.016.

Van Deventer, J.A., Kelly, R.L., Rajan, S., Wittrup, K.D., and Sidhu, S.S. (2015). A switchable yeast display/secretion system. Protein Eng Des Sel *28*, 317–325. https://doi.org/10.1093/protein/gzv043.

Van Deventer, J.A., Le, D.N., Zhao, J., Kehoe, H.P., and Kelly, R.L. (2016). A platform for constructing, evaluating, and screening bioconjugates on the yeast surface. Protein Eng Des Sel *29*, 485–494. https://doi.org/10.1093/protein/gzw029.

Vanderschuren, K., Arranz-Gibert, P., Khang, M., Hadar, D., Gaudin, A., Yang, F., Folta-Stogniew, E., Saltzman, W.M., Amiram, M., and Isaacs, F.J. (2022). Tuning protein half-life in mouse using sequence-defined biopolymers functionalized with lipids. PNAS *119*. https://doi.org/10.1073/pnas.2103099119.

Vargas-Rodriguez, O., Sevostyanova, A., Söll, D., and Crnković, A. (2018). Upgrading aminoacyl-tRNA synthetases for genetic code expansion. Current Opinion in Chemical Biology *46*, 115–122. https://doi.org/10.1016/j.cbpa.2018.07.014.

Venkat, S., Sturges, J., Stahman, A., Gregory, C., Gan, Q., and Fan, C. (2018). Genetically Incorporating Two Distinct Post-translational Modifications into One Protein Simultaneously. ACS Synth. Biol. *7*, 689–695. https://doi.org/10.1021/acssynbio.7b00408.

Wang, K., Sachdeva, A., Cox, D.J., Wilf, N.M., Lang, K., Wallace, S., Mehl, R.A., and Chin, J.W. (2014). Optimized orthogonal translation of unnatural amino acids enables spontaneous protein double-labelling and FRET. Nature Chem *6*, 393–403. https://doi.org/10.1038/nchem.1919.

Wang, Q., Parrish, A.R., and Wang, L. (2009). Expanding the Genetic Code for Biological Studies. Chemistry & Biology *16*, 323–336. https://doi.org/10.1016/j.chembiol.2009.03.001.

Willis, J.C.W., and Chin, J.W. (2018). Mutually orthogonal pyrrolysyl-tRNA synthetase/tRNA pairs. Nature Chem *10*, 831–837. https://doi.org/10.1038/s41557-018-0052-5.

Wiltschi, B. (2016). Incorporation of non-canonical amino acids into proteins in yeast. Fungal Genetics and Biology *89*, 137–156. https://doi.org/10.1016/j.fgb.2016.02.002.

Winz, M.L., Linder, E.C., Becker, J., and Jäschke, A. (2018). Site-specific one-pot triple click labeling for DNA and RNA. Chem. Commun. *54*, 11781–11784. https://doi.org/10.1039/C8CC04520H.

Wu, B., Wang, Z., Huang, Y., and Liu, W.R. (2012). Catalyst-Free and Site-Specific One-Pot Dual-Labeling of a Protein Directed by Two Genetically Incorporated Noncanonical Amino Acids. ChemBioChem *13*, 1405–1408. https://doi.org/10.1002/cbic.201200281.

Wu, N., Deiters, A., Cropp, T.A., King, D., and Schultz, P.G. (2004). A Genetically Encoded Photocaged Amino Acid. J. Am. Chem. Soc. *126*, 14306–14307. https://doi.org/10.1021/ja040175z.

Xiao, H., Chatterjee, A., Choi, S., Bajjuri, K.M., Sinha, S.C., and Schultz, P.G. (2013). Genetic Incorporation of Multiple Unnatural Amino Acids into Proteins in Mammalian Cells. Angewandte Chemie International Edition *52*, 14080–14083. https://doi.org/10.1002/anie.201308137.

Xu, H., Wang, Y., Lu, J., Zhang, B., Zhang, Z., Si, L., Wu, L., Yao, T., Zhang, C., Xiao, S., et al. (2016). Re-exploration of the Codon Context Effect on Amber Codon-Guided Incorporation of Noncanonical Amino Acids in Escherichia coli by the Blue–White Screening Assay. ChemBioChem *17*, 1250–1256. https://doi.org/10.1002/cbic.201600117.

Zackin, M.T., Stieglitz, J.T., and Deventer, J.A.V. (2022). Genome-wide screen for enhanced noncanonical amino acid incorporation in yeast. bioRxiv. https://doi.org/10.1101/2022.04.28.489958.

Zheng, Y., Addy, P.S., Mukherjee, R., and Chatterjee, A. (2017). Defining the current scope and limitations of dual noncanonical amino acid mutagenesis in mammalian cells. Chem. Sci. *8*, 7211–7217. https://doi.org/10.1039/C7SC02560B.

Zheng, Y., Mukherjee, R., Chin, M.A., Igo, P., Gilgenast, M.J., and Chatterjee, A. (2018a). Expanding the Scope of Single- and Double-Noncanonical Amino Acid Mutagenesis in Mammalian Cells Using Orthogonal Polyspecific Leucyl-tRNA Synthetases. Biochemistry *57*, 441–445. https://doi.org/10.1021/acs.biochem.7b00952.

Zheng, Y., Gilgenast, M.J., Hauc, S.C., and Chatterjee, A. (2018b). Capturing post-translational modification-triggered protein-protein interactions using dual noncanonical amino acid mutagenesis. ACS Chem Biol *13*, 1137–1141. https://doi.org/10.1021/acschembio.8b00021.

Zubi, Y.S., Seki, K., Li, Y., Hunt, A.C., Liu, B., Roux, B., Jewett, M.C., and Lewis, J.C. (2022). Metal-responsive regulation of enzyme catalysis using genetically encoded chemical switches. Nat Commun *13*, 1864. https://doi.org/10.1038/s41467-022-29239-y.